Running head: Introgression in hares

Title: The legacy of recurrent introgression during the radiation of hares

Mafalda S. Ferreira[1,2,3], Matthew R. Jones[3], Colin M. Callahan[3], Liliana Farelo[1], Zelalem Tolesa[4], Franz Suchentrunk[5], Pierre Boursot[6], L. Scott Mills[7,8,9], Paulo C. Alves[1,2,7], Jeffrey M. Good[3,7,*], José Melo-Ferreira[1,2,*]

[1]*CIBIO, Centro de Investigação em Biodiversidade e Recursos Genéticos, InBIO Laboratório Associado, Universidade do Porto, Vairão, Portugal.*

[2]*Departamento de Biologia, Faculdade de Ciências da Universidade do Porto, Porto, Portugal.*

[3]*Division of Biological Sciences, University of Montana, Missoula, Montana, USA.*

[4]*Department of Biology, Hawassa University, Hawassa, Ethiopia.*

[5]*Research Institute of Wildlife Ecology, University of Veterinary Medicine Vienna, Vienna, Austria.*

[6]*Institut des Sciences de l'Évolution Montpellier (ISEM), Université Montpellier, CNRS, IRD, EPHE, France.*

[7]*Wildlife Biology Program, College of Forestry and Conservation, University of Montana, Missoula, Montana, USA.*

[8]*Office of Research and Creative Scholarship, University of Montana, Missoula, Montana, USA.*

[9]*Fisheries, Wildlife, and Conservation Biology Program, Department of Forestry and Environmental Resources, North Carolina State University, Raleigh, North Carolina, USA.*

*Shared senior authorship.

Correspondence: Mafalda S. Ferreira, mafaldasferreira@cibio.up.pt; Jeffrey M. Good, jeffrey.good@umontana.edu; José Melo-Ferreira, jmeloferreira@cibio.up.pt

ABSTRACT

Hybridization may often be an important source of adaptive variation, but the extent and long-term impacts of introgression have seldom been evaluated in the phylogenetic context of a radiation. Hares (*Lepus*) represent a widespread mammalian radiation of 32 extant species characterized by striking ecological adaptations and recurrent admixture. To understand the relevance of introgressive hybridization during the diversification of *Lepus*, we analyzed whole exome sequences (61.7 Mb) from 15 species of hares (1- 4 individuals per species), spanning the global distribution of the genus, and two outgroups. We used a coalescent framework to infer species relationships and divergence times, despite extensive genealogical discordance. We found high levels of allele sharing among species and show that this reflects extensive incomplete lineage sorting and temporally layered hybridization. Our results revealed recurrent introgression at all stages along the *Lepus* radiation, including recent gene flow between extant species since the last glacial maximum, but also pervasive ancient introgression occurring since near the origin of the hare lineages. We show that ancient hybridization between northern hemisphere species has resulted in shared variation of potential adaptive relevance to highly seasonal environments, including genes involved in circadian rhythm regulation, pigmentation, and thermoregulation. Our results illustrate how the genetic legacy of ancestral hybridization may persist across a radiation, leaving a long-lasting signature of shared genetic variation that may contribute to adaptation within and among species.

KEYWORDS

Ancient introgression; Adaptation; Hybridization; Phylogenomics; *Lepus*

Species radiations are often accompanied by extensive gene flow between nascent lineages (e.g., Lamichhaney et al. 2015; Árnason et al. 2018; Malinsky et al. 2018; Li et al. 2019; Barth et al. 2020). Genetic signatures of hybridization between several closely related species could either represent recent or ongoing introgressive hybridization (Eaton et al. 2015), or the remnants of hybridization among ancestral populations that remain shared among contemporary species (Malinsky et al. 2018; Li et al. 2019). Although these alternatives can be difficult to differentiate in large radiations (Eaton et al. 2015; Malinsky et al. 2018; Vanderpool et al. 2020), both ancient and contemporary introgression has been linked to local adaptation in several systems (e.g., Liu et al. 2015; Gittelman et al. 2016; Meier et al. 2017; Barlow et al. 2018; Giska et al. 2019; Svardal et al. 2020). Thus, unraveling the tempo and contribution of introgression to standing genetic variation within and among species remains a critical step in understanding the overall importance of introgression to evolution.

Reconstructing the history of hybridization between several closely related species requires inferring evolutionary relationships among species while considering the two primary processes – incomplete lineage sorting and gene flow – that may cause sharing of genetic variation among populations (Malinsky et al. 2018). The network multispecies coalescent (NMSC) model (Than et al. 2011; Solís-Lemus et al. 2017; Degnan 2018) offers one promising framework that appears to resolve species relationships in the face of multiple reticulation events and rapid speciation (Kozak et al. 2018; Edelman et al. 2019). However, the NMSC is still prohibitive for large

76 datasets and choosing the exact number of migration events is not straightforward (Yu
77 and Nakhleh 2015). Alternatively, site-based summary statistics based on tree
78 asymmetries (e.g., Green et al. 2010; Pease and Hahn 2015), or admixture proportions
79 (e.g., Reich et al. 2009; Martin et al. 2015; Malinsky et al. 2018) are simpler to
80 implement, but offer less power for localizing the timing and number of introgression
81 events when recurrent hybridization is layered across a phylogeny (Malinsky et al.
82 2018). A combination of methods is thus most appropriate to infer a species tree that
83 may have layered events of hybridization throughout time (e.g., Kozak et al. 2018;
84 Malinsky et al. 2018; Edelman et al. 2019; Li et al. 2019).

85 Hares and jackrabbits comprise a group of 32 species (genus *Lepus*; Smith et al.
86 2018) whose common ancestor likely originated in North America and spread
87 throughout most of the Northern Hemisphere and Africa presumably in the last 4-6
88 million years (Yamada et al. 2002; Matthee et al. 2004; Melo-Ferreira et al. 2012).
89 Hares are primarily associated with open grasslands, but can be found across a broad
90 range of biomes (e.g., desert, forest, or arctic) and elevations (e.g., from sea level to the
91 Himalayan or Ethiopian plateau; Smith et al., 2018). The *Lepus* radiation also provides
92 case studies of hybridization and introgression, since admixture has been detected
93 among several modern species pairs (e.g., Liu et al. 2011; Melo-Ferreira et al. 2012;
94 Tolesa et al. 2017; Jones et al. 2018; Seixas et al. 2018; Lado et al. 2019; Kinoshita et
95 al. 2019). Selection on introgressed variation has been hypothesized to have aided the
96 range expansion of the Iberian hare (Seixas et al. 2018), and has been directly linked to
97 convergent adaptive evolution of non-white winter coats in populations of two species
98 that change the color of their pelage seasonally (Jones et al. 2018; Giska et al. 2019;
99 Jones et al. 2020a). These studies suggest that the relatively recent exchange of genetic
100 variation among extant *Lepus* species has provided an important source of adaptive

variation. However, the phylogenetic relationships among *Lepus* species remain poorly resolved (Halanych et al. 1999; Matthee et al. 2004; Melo-Ferreira et al. 2012; Melo-Ferreira and Alves 2018), and the contribution of ancient gene flow to the *Lepus* evolutionary history in a deeper phylogenetic context remains unknown.

Here, we use exome-wide data to infer the evolutionary history of 15 *Lepus* species and show that hybridization between lineages has likely occurred since the origin of the radiation. The combination of incomplete lineage sorting and these temporally layered events of hybridization have resulted in extremely high levels of shared genetic variation among extant species, including species that currently occur on different continents. We then use the case of ancient admixture among northern latitude species that occupy highly seasonal environments to investigate the gene content and possible functional relevance of introgressed genomic regions. Our work demonstrates that recurrent introgression throughout evolutionary history has made a substantial contribution to genetic variation within and among species of this widespread mammalian radiation.

MATERIALS AND METHODS

Taxon Sampling and Exome Sequencing

We generated new genome-wide resequencing data targeting 207,691 exonic and non-coding regions [totaling 61.7 Megabases (Mb) total] from 14 hare species (30 individuals) and the outgroup pygmy rabbit (*Brachylagus idahoensis*; 2 individuals). We combined these data with published whole exomes from four snowshoes hares [*Lepus americanus*; NCBI Sequence Read Archive BioProject PRJNA420081 from Jones et al. (2018, 2020b)] and extracted data from the reference genome of European rabbit (*Oryctolagus cuniculus*; OryCun2.0; Carneiro *et al.*, 2014) to use as second

126 outgroup. Our total sample of 15 hare species (34 individuals, 1 to 4 individuals per
127 species) and 2 outgroup species (3 individuals) included species from all major regions
128 of the *Lepus* native distribution: Africa (3 species), Africa and Eurasia (1 species),
129 Eurasia (6 species) and North America (5 species) (Fig. 1 and Supplementary Table S1).
130 Exome capture experiments were performed following the procedures outlined
131 in Jones et al. (2018) and in the Appendix. Briefly, we obtained samples as tissue or
132 extracted DNA including samples from previous studies or through loans from
133 collaborators (Supplementary Table S1). Depending on the sample, genomic DNA was
134 isolated using a saline extraction method (Sambrook et al. 1989) or DNeasy Blood &
135 Tissue Kit (Qiagen) (Supplementary Table S1 and Appendix). We prepared Illumina
136 sequencing libraries for each sample following Meyer and Kircher (2010) with minor
137 modifications [see Appendix and Jones et al. (2018)]. Sequencing libraries were then
138 enriched using NimbleGen SeqCap EZ v.4.3 protocol and a custom capture design
139 consisting of 213,164 probes targeting ~25 Mb of protein-coding exons, ~28 Mb of
140 untranslated regions, and ~9 Mb of intron/intergenic regions (Jones et al. 2018).
141 Hybridization reactions were performed in two separate equimolar pools of indexed
142 libraries (31 and 29 libraries, Supplementary Table S1), together with samples used for
143 other studies. The target enriched pools were each sequenced across two lanes of an
144 Illumina HiSeq1500 sequencer (125 bp paired-end reads) at CIBIO-InBIO's New-Gen
145 sequencing platform, Portugal.
146
147 *Read Processing and Genotyping*
148 We trimmed adapters, low-quality bases, merged overlapping reads, and
149 removed PCR duplicates from raw reads using the *expHTS* pipeline (v.0.Mar112016;
150 https://github.com/msettles/expHTS). We then used *pseudo-it* (v1; Sarver et al. 2017) to

151 generate pseudo-reference exomes for each species by iteratively mapping (four
152 iterations and allowing ambiguity codes) cleaned single and paired-end reads from one
153 individual per species (Supplementary Table S1) to the rabbit reference genome
154 (OryCun2.0) (Carneiro et al. 2014). For snowshoe hares and black-tailed jackrabbits, we
155 used pseudo-references generated by Jones et al. (2018).

156 We then mapped data from all individuals to each species-specific pseudo-
157 reference using *bwa-mem* (v.0.7.12-r1039; Li 2013) with default options. Mapped reads
158 were sorted with *samtools* (v1.4; Li et al. 2009), assigned to read groups, filtered for
159 duplicates (*Picard* v1.140; http://broadinstitute.github.io/picard/), and realigned for
160 insertion-deletion length variation using GATK (v3.4.46; Van der Auwera et al. 2013).
161 We calculated coverage statistics and capture efficiency using *CalculateHSMetrics* from
162 *Picard*. For each individual, we called and filtered genotypes using the *bcftools* (v1.4;
163 Li 2011) mpileup, call and filter pipeline and used the curated genotypes to construct
164 consensus exome fasta sequences in the OryCun2.0 coordinate system (see Appendix
165 for more details on the filtering pipeline). Many of the steps of the bioinformatics
166 pipeline in our analyses benefited from parallelization provided by GNU parallel (Tange
167 2011).

168

169 *Species Tree Inference*

170 We used a concatenated alignment to estimate a single bifurcating phylogeny using a
171 maximum likelihood (ML) search and rapid bootstrapping run under the GTR+Γ model
172 of sequence evolution (autoMRE option) in *RAxML* (v8.2.10; Stamatakis 2018). We
173 then used two complementary methods to infer multispecies-coalescent trees while
174 accounting for local variation in phylogenetic histories along the genome. First, we
175 extracted alignments from the targeted regions and 200 base pairs (bp) of flanking

176 sequences across 50 kilobase (kb) genomic intervals, considering a balance between the
177 expected extent of LD in hares (10-20 kb; Jones et al. 2018) and the retention of
178 information for phylogenetic analysis (alignment length > 1 kb). For each window, we
179 filtered positions with missing data for > 30% of individuals using *TriSeq* (*TriFusion*
180 *1.0.0;* http://odiogosilva.github.io/TriFusion/), excluded windows smaller than 1 kb, and
181 used *RAxML* to estimate local maximum likelihood trees (GTR+Γ, 100 bootstraps) and
182 corresponding tree certainty scores. We then used all windows with tree certainty scores
183 above 5. The tree certainty score is the sum of certainty scores for all internodes of a
184 tree. The internode certainty score weighs the support of the bipartition represented by a
185 given internode against the support of the second most prevalent conflicting bipartition
186 (Salichos et al. 2014). In our case, the maximum theoretical value of the tree certainty
187 score is 31, or k – 3 with k equal to the number of taxa (Salichos et al. 2014). We
188 unrooted the gene trees using R package *ape* (Paradis et al. 2004) to estimate a
189 consensus species tree using *ASTRAL-III* (5.6.3; Zhang et al. 2018).

190 We also estimated coalescent species trees using only variable sites with
191 *SVDquartets* (Chifman and Kubatko 2014) implemented in *PAUP** (4a163; Swofford
192 2003). For the analyses based on variable sites, we recovered single nucleotide variants
193 (SNVs) distanced 10 kb along the genome, and excluded sites with missing information
194 for >30% of the individuals. For both *SVDquartets* and *ASTRAL* analyses, species trees
195 were estimated with and without assigning species identities and using sites/intervals
196 genome-wide or only from the X chromosome. The European and/or pygmy rabbits
197 were included for all analyses requiring outgroups. Additional details on the
198 phylogenetic analyses are provided in the Appendix.

199

200 *Bayesian Divergence Time Inference*

201 We performed Bayesian inference of divergence times in the inferred species tree using
202 an approximate maximum likelihood method and assuming an autocorrelated relaxed
203 molecular clock, implemented in *MCMCtree* (*PAML v.4.9*; Yang 2007) and described
204 in dos Reis and Yang (2011, 2019). For one individual per species (Supplementary
205 Table S1), we extracted the coding sequence for all genes included in our capture design
206 (18,798 genes in the OryCun2.0 ENSEMBLE 94 database), selecting the longest
207 transcript per gene using R package *biomaRt* (v2.34.2; Durinck et al. 2005, 2009) and
208 excluding alignments with more than 20% missing data using *AMAS* (Borowiec 2016)
209 (see Appendix for details). With these, we constructed a concatenated alignment with
210 three partitions, corresponding to the three codon positions. We assumed GTR+Γ for
211 the model of sequence evolution, we used the prior of 3.33 for the average substitution
212 rate per site per 100 million years, following Matthee et al. (2004). We discarded the
213 first 1,000,000 samples as burn-in and ran the program until we gathered 1,000,000
214 samples from the posterior, sampling every 10 iterations, and repeated the analysis
215 twice to ensure convergence. We checked for convergence between the two runs by
216 confirming a linear correlation between posterior times, trendless trace plots, and high
217 effective sample size (ESS) values following dos Reis and Yang (2019). Finally, we
218 also checked for a linear relationship between posterior times and confidence interval
219 widths in infinite sites plots (Inoue et al. 2010).

220 *Lepus* is poorly represented in the fossil record. The earliest hare record dates to
221 the early Pleistocene (2.5 million years ago; Ma) (White 1991; Lopez-Martinez 2008),
222 which is much more recent than molecular estimates for the genus extrapolated from
223 deeper fossil calibrations (4-6 Ma; Yamada et al. 2002). Therefore, we dated the species
224 tree either (1) using previous molecular estimates of 4-6 Ma for *Lepus* diversification
225 extrapolated from deep fossil record calibrations of the order Lagomorpha (Yamada et

226 al. 2002) and 9.7-14.5 Ma for the *Oryctolagus-Lepus* divergence (Matthee et al. 2004)
227 or (2) using the fossil estimates of 2.5 Ma for the lower bound of *Lepus* diversification,
228 and constraining this node to be no older than 4.8 Ma, which is when the fossil record
229 suggests that the common ancestor of Leporids (rabbits and hares) existed (Hibbard
230 1963; White 1991).
231
232 *Ancestral Range Reconstruction*
233 We reconstructed ancestral continental ranges for *Lepus* using the likelihood
234 reconstruction method (Schluter et al. 1997; Pagel 1999) implemented in *Mesquite*
235 (v3.51; Maddison and Maddison 2018). We generated a character matrix coding each
236 species as being distributed in North America (0), Eurasia (1) or Africa (2). Even
237 though the Cape hare *sensu lato* is distributed in Africa and Eurasia, Lado et al. (2019)
238 showed deep divergence and non-monophyly of African and Eurasian lineages. Because
239 our Cape hare samples represent the African lineage, we assigned the Cape hare
240 distribution to Africa. We used the Markov k-state one-parameter model (Mk1) (Lewis
241 2001) and the rooted topology and branch-lengths of the concatenated ML tree to infer
242 ancestral states of internal nodes. Nodes for which the decision threshold differed by
243 less than 2.0 between states were considered ambiguous.
244
245 *Gene Tree Discordance and Phylogenetic Networks*
246 To explore the amount and effect of gene tree discordance in our dataset, we performed
247 a series of analyses. First, we produced a split network using all gene trees previously
248 used as input for *ASTRAL* (tree certainty scores > 5) using *SplitsTree4* (v4.14.6; Huson
249 and Bryant 2006) with the option "Consensus Network with distances as means" and a
250 5% threshold. We also used the same set of gene trees (tree certainty scores > 5) to

251 produce a majority rule consensus tree with *RAxML* (-L MRE option), including
252 internode certainty scores (Salichos et al. 2014). We then used *DiscoVista* (Sayyari et
253 al. 2018) to plot *ASTRAL* quartet frequencies around nodes of interest. Finally, we
254 calculated Robinson-Foulds normalized distances between gene trees and the *ASTRAL*
255 species tree where individuals are not assigned to species, and among gene trees using
256 the function *RF.dist()* from the R package *phangorn* (2.4.0 ;Schliep 2011). This metric
257 varies between 0 (no discordance between trees) and 1 (complete discordance).
258 We used *PhyloNet* (v3.6.6; Yu and Nakhleh 2015) to model species
259 relationships under the network multispecies coalescent model, using all local
260 genealogies (tree certainty scores > 5). We ran *InferNetwork_MPL* (Yu and Nakhleh
261 2015) with 0 to 4 migration events, associating individuals to species (option -a), and
262 optimizing branch lengths and inheritance probabilities to compute likelihoods for each
263 proposed network (option -o). We used the best likelihoods per run to calculate
264 Bayesian Information Criteria (BIC) and Akaike information criteria corrected for small
265 samples sizes (AICc) following (Yu et al. 2012, 2014) to compare the resulting
266 networks. Networks were visualized with *IcyTree* (https://icytree.org; last accessed July
267 2019). We also reconstructed ancestral population graphs with *TreeMix* (v1.13, options
268 -global, -noss and -se; Pickrell and Pritchard 2012) based on the SNV dataset used for
269 *SVDQuartets*. We allowed 0 to 9 migration events and used the white-sided jackrabbit
270 (*Lepus callotis*) as the outgroup relative to all other *Lepus* species (see *Results*).
271
272 *Genetic Diversity, Divergence, and Admixture*
273 We used the *genomics general* toolkit (https://github.com/simonhmartin/; last accessed
274 January 14, 2019) to estimate pairwise genetic distances between species and nucleotide
275 diversity within species, and a custom script (available at https://github.com/evochange)

to calculate the number of heterozygous sites per individual and the subset shared among species. All diversity estimates were based on a genome-wide concatenated alignment, where we excluded sites with missing information for >30% of the individuals.

We then used *genomics general* and custom scripts (available at https://github.com/evochange) to calculate several variants of the D-statistics (Green et al. 2010) from the informative sites in the same filtered alignment, treating the European rabbit sequence as the ancestral state (additional details are provided in the Appendix). Briefly, we calculated the minimum absolute value of D (D_{min}) (Malinsky et al. 2018) for all possible species trios. We calculated z-scores for each D value using a 1 Mb block jackknife approach. After finding the minimum D per trio, D values with Bonferroni-corrected $P \leq 0.05$ were considered significantly different from zero. We then calculated the 'f-branch' statistic ($f_b(C)$) (Malinsky et al. 2018). The 'f-branch' statistic measures admixture proportion between species *C* and branch *b* by calculating admixture proportion among all possible *f*(A,B,C,O) combinations where *A* are all descendants of branch *a* (sister to *b*), *B* are all descendants of branch *b*, and *C* is the donor taxa. $f_b(C)$ is the minimum *f* value across all possible *B* and the median across all possible *A*. A significant $f_b(C)$ value means that all descendants *B* of branch *b* share alleles with *C,* which is more parsimoniously explained by an event of ancestral introgression from *C* to *b* (Malinsky et al. 2018). Using the inferred species tree, we determined all conformations (A,B;C,O) needed to calculate $f_b(C)$ for all pairs of *C* species and *b* branches following Malinsky et al. (2018), custom scripts (available at https://github.com/evochange) and R package *treeman* (1.1.3; Bennett et al. 2017). For each conformation, we calculated 'admixture proportion' (f_G) as defined in Martin et al. (2015) and Malinsky et al. (2018) and z-scores with 1 Mb block jackknife approach

301 following Malinsky et al. (2018). We also calculated f_{hom} (Martin et al. 2015) between
302 black-tailed jackrabbits (P3) and several snowshoe hare populations (as P1 and P2) to
303 evaluate levels of admixture estimated with $f_b(C)$ for this species pair (see *Results* and
304 *Discussion*).

305 We also estimated the fraction of admixture (f_d) (Martin et al. 2015) across 50 kb
306 genomic sliding windows (≥100 sites, 5 kb steps), to localize introgression in the
307 genomes of northern latitude species (snowshoe hares, mountain hares, Alaskan hares,
308 and white-tailed jackrabbits). We performed three scans testing introgression between
309 snowshoe hares (P3) and Alaskan hares, mountain hares or white-tailed jackrabbits
310 (alternative P2), using the Iberian hare as P1. Windows of top 0.5% f_d were considered
311 significant. Following Liu et al. (2015), we considered that significant windows in all
312 three tests reflected introgression between snowshoe hares and the ancestral lineage of
313 white-tailed jackrabbits/mountain hares/Alaskan hares, while significant windows in
314 only one test result from recent introgression between the focal extant species. We
315 obtained the annotation of genes in these windows from the rabbit reference and
316 performed an enrichment analysis in *g:Profiler* (accessed September 2019; Raudvere et
317 al. 2019) using default parameters. We also calculated d_{xy} for f_d outlier windows and the
318 exome-wide d_{xy} distribution between the focal pair of P2-P3 species.

319

320 **RESULTS**

321 *Whole Exome Sequencing Data*

322 We analyzed whole exome sequence data (61.7Mb) from 15 hare species and two
323 outgroups, combining newly generated (30 individuals from 14 hare species and 2
324 individuals from the outgroup pygmy rabbit) and published data (4 individuals from 1
325 additional hare species and the outgroup European rabbit; Carneiro et al. 2014; Jones et

326 al. 2018, 2020b) (Supplementary Table S1). Custom DNA captures showed high
327 efficiency (32.3 average fold-enrichment) and specificity (average 10% of sequenced
328 bases off-target; Supplementary Table S2). Mapping cleaned reads onto species-specific
329 pseudo-references resulted in an average target sequencing coverage of 16× (5-35× on
330 average per sample; Supplementary Table S2) with 57.8 million genotyped sites per
331 individual (Supplementary Table S2). Two lower coverage individuals (one hare
332 individual and one pygmy rabbit individual) and one locality duplicate (one hare) were
333 removed from the final dataset to maximize data quality and avoid geographic
334 redundancy (Supplementary Table S1). All analyses were performed on a dataset of 15
335 hare species (32 individuals), one pygmy rabbit, and the rabbit reference genome, unless
336 otherwise noted (see Supplementary Table S1).
337
338 *Phylogenetic Relationships among Hares*
339 The overall topologies of the concatenated ML phylogeny (11,949,529 positions with
340 no missing data) and the multispecies-coalescent species trees of *ASTRAL* (8,889 gene
341 trees estimated from 50 kb genomic intervals; alignment lengths between 1 kb and 29
342 kb) and *SVDquartets* (45,779 unlinked SNPs) were largely concordant (Supplementary
343 Figs. S1, S2 and S3). Branching relationships were highly supported in general
344 (*ASTRAL* posterior probabilities equal to 1 and *SVDquartets* bootstrap supports > 90),
345 except for i) the placement of European hares (*L. europaeus*) as sister to the clade of
346 African species, and ii) the sister relationship of the Iberian hare (*L. granatensis*) and
347 the clade containing the white-tailed jackrabbit (*L. townsendii*), Alaskan and mountain
348 hares (Fig. 1 and Supplementary Figs. S1, S2, S3 and S4). Even though the taxonomy of
349 some hare species has been controversial (e.g., Halanych et al. 1999; Alves et al. 2008;
350 Melo-Ferreira and Alves 2018; Lado et al. 2019), our analyses recovered most species

351 as monophyletic (Supplementary Figs. S1, S2a and S3a). Possible exceptions were the
352 potential paraphyly of the mountain hare (*L. timidus*) with the Alaskan hare (*L. othus*)
353 (suggested by *ASTRAL* and *SVDquartets*; Supplementary Figs. S2a and S3a) and of the
354 broom hare (*L. castroviejoi*) with the Corsican hare (*L. corsicanus*) (recovered with
355 *ASTRAL*; Supplementary Fig. S2a). Both these cases involve sister taxa that likely share
356 a very recent common ancestor and for which the classification as separate species has
357 been debated (Alves et al. 2008; Melo-Ferreira et al. 2012). Also, we consistently
358 estimated paraphyly of the Cape hare (*L. capensis*) with the Ethiopian hare (*L. fagani*),
359 with the North African Cape hare specimen sharing a more recent common ancestor
360 with Ethiopian hares than the South African Cape hare specimen (Supplementary Figs.
361 S1, S2a and S3a). This may result from the known deep intraspecific divergences and
362 paraphyly of Cape hare lineages (Lado et al. 2019), confirmed by our diversity and
363 divergence estimates (Supplementary Tables S3 and S4).

364 Dating the species tree using either molecular-based dates extrapolated from
365 deep fossil calibrations (Yamada et al. 2002; Matthee et al. 2004) or *Lepus* fossil record
366 calibrations (Hibbard 1963; White 1991) recovered overlapping 95% high posterior
367 density (HPD) intervals of divergence times for relatively recent splits (e.g.,
368 diversification of Eurasian and African species; Supplementary Table S5). However,
369 *Lepus*-based fossil calibrations suggested more recent ages for deeper nodes
370 (Supplementary Table S5 and Fig. S5). For instance, dates extrapolated from deeper
371 fossil calibrations outside of *Lepus* sets the base of the hare radiation at ~5.83 million
372 year ago (Ma) (95% HPD 6.17-5.34 Ma), whereas *Lepus* fossil calibration recovered
373 ~4.05 Ma (95% HPD 5.00-3.18 Ma). All analyses were consistent in showing that the
374 deepest branching events involved North American species: white-sided jackrabbit (*L.*
375 *callotis*), black-tailed jackrabbit, and snowshoe hare (*L. americanus*) (Fig. 1b). In

accordance, ancestral reconstruction of biogeographic distributions (Fig. 1c and Supplementary Table S6) supported an initial radiation of the genus in North America, with subsequent colonization of Eurasia (2.85 and 1.99 Ma for deeper and *Lepus*-fossil calibration, respectively) and Africa (1.85 and 1.33 Ma for deeper and fossil calibration, respectively). The North America distribution of white-tailed jackrabbits and Alaskan hares (Fig. 1a) likely results from one or two re-colonization events from Eurasia (Fig. 1c and Supplementary Table S6). These results also confirm the paraphyly of the jackrabbit species (Halanych et al. 1999).

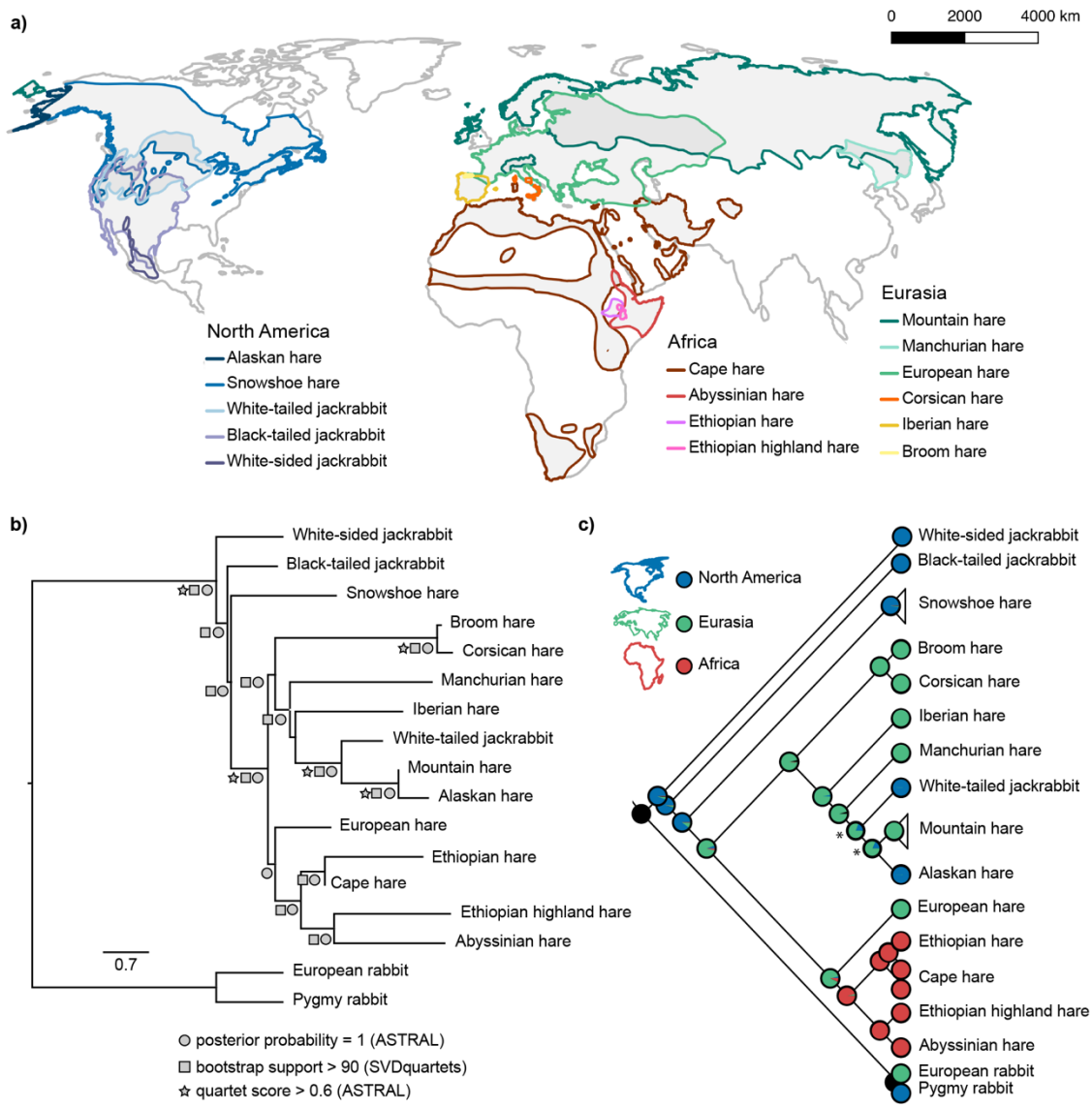

385 **Fig. 1 - Hare (*Lepus* spp.) evolutionary history and biogeography. A)** The
386 distribution of the 15 hare species studied here; **B)** Coalescent species tree estimated
387 with *ASTRAL;* nodes with *ASTRAL* posterior probability equal to one, *ASTRAL* quartet
388 score higher than 0.6, and *SVDquartets* bootstrap support higher than 90 are labeled; **C)**
389 Maximum-likelihood phylogeny of *Lepus* showing ancestral range reconstructions. Pie
390 charts show proportional likelihoods that the common ancestral was distributed in North
391 America (blue), Eurasia (green) or Africa (red). Asterisks depict nodes with equivocal
392 reconstruction of ancestor distribution.
393
394 *Incomplete Lineage Sorting and Introgression*
395 We recovered a highly supported species trees across phylogenetic methods, albeit with
396 extensive phylogenetic discordance among sequenced regions [average Robinson-
397 Foulds (RF) pairwise distance between local trees was 0.73]. No local tree completely
398 recovered the species tree topology (minimum RF distance between gene and species
399 tree was 0.13) (Supplementary Fig. S6) and the majority rule consensus tree showed
400 low internode certainty (Supplementary Fig. S7). Extensive phylogenetic discordance
401 was also apparent in the *ASTRAL* species tree with all but three branches showing
402 quartet scores below 0.6 (Fig. 1, Supplementary Figs. S2, S4 and Tables S7 and S8).
403 Splits network analysis of individual gene trees also supported many alternative
404 relationships (represented by cuboid structures connecting alternative topologies)
405 particularly involving deeper branches (Fig. 2). We estimated similar levels of
406 discordance between X-linked and autosomal genealogies and the inferred species trees
407 (Supplementary Fig. S6). Furthermore, a species tree inferred with X-linked data
408 differed from the genome-wide species tree and showed lower overall branch support
409 (Supplementary Fig. S8 and Table S9). Measures of intraspecific diversity were

410 relatively low within species [π between 0.13% (Corsican hare) and 0.63% (black-tailed
411 jackrabbit] but overlapped in range with estimates of absolute genetic divergence
412 between species [d_{xy} between 0.17% (broom hare and Corsican hare) and 1.11%
413 (snowshoe hare and white-sided jackrabbit)] (Supplementary Tables S3 and S4). Some
414 instances of low interspecific divergence reflect sister taxa where the species-level
415 designations have been debated (e.g., the Corsican-Broom hare and Mountain-Alaskan
416 hare complexes; Alves et al. 2008; Melo-Ferreira et al. 2012). Alternatively, high
417 intraspecific diversity may reflect cryptic divergence within recognized species (e.g.,
418 snowshoe hares, Melo-Ferreira et al. 2014; Cape hares, Lado et al. 2019).

419 On average, 49% of heterozygous sites in individuals of one species were shared
420 with individuals from at least one other species (Supplementary Table S10). Such high
421 levels of shared polymorphism between species coupled with extensive phylogenetic
422 discordance across the genome could be explained by recent rapid speciation leading to
423 extensive incomplete lineage sorting, secondary introgression between lineages, or a
424 mixture of both processes. To differentiate these alternatives, we first tested if the
425 proportions of shared-derived variants between species across the genome supported a
426 strictly bifurcating history (expected with incomplete lineage sorting) by calculating
427 minimum absolute D-statistics (D_{min}) (Malinsky et al. 2018) for all trios of species in
428 our dataset. We found that 88% of these comparisons were significantly different from
429 zero (Bonferroni-corrected $P < 0.05$; Supplementary Fig. S9). This suggests that the
430 level of shared alleles among the majority of species trios is incompatible with a single
431 tree (even accounting for incomplete lineage sorting), providing overwhelming support
432 for gene flow among species. This striking pattern of introgression could be driven by
433 rampant gene flow among extant species pairs, or represent signatures of introgression
434 between ancestral lineages that remain in modern species (Malinsky et al. 2018).

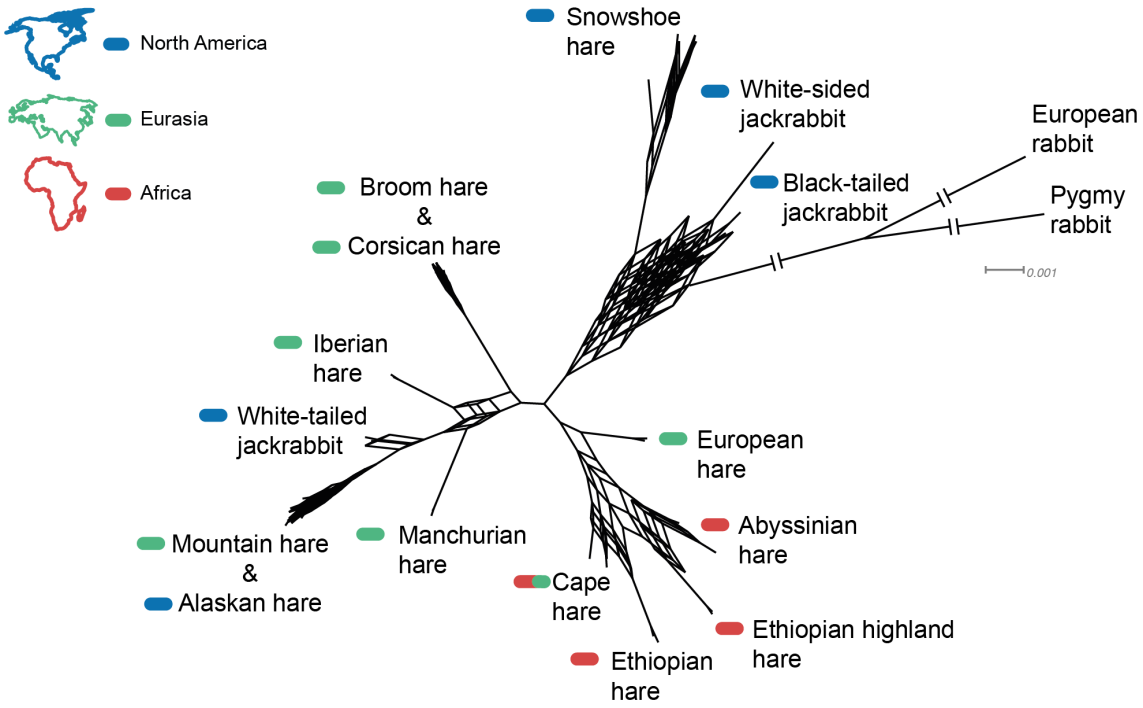

Fig. 2 - The hare (*Lepus* spp.) species tree is underlined by extensive gene tree incongruence. Splits network constructed from 8889 gene trees (5% threshold) shows discordance among the gene tree topologies (cuboid structures represent alternative topologies) in deeper nodes of the species tree. Species are marked with colors corresponding to the continents where they are distributed.

To disentangle temporally layered signatures of introgression, we combined analyses based on the multispecies network coalescent implemented in *PhyloNet* (Yu and Nakhleh 2015) (Supplementary Fig. S10), ancestral population graph reconstruction with *TreeMix* (based on 30,709 biallelic SNVs; Supplementary Figs. S11 and S12; Pickrell and Pritchard 2012), and estimates of admixture proportions among species based on the 'f-branch' metric ($f_b(C)$) (Malinsky et al. 2018) (Fig. 3). Collectively, our results were consistent with recurrent gene flow between species layered across the diversification of *Lepus*. We detected introgression among extant species pairs within all of the major geographic regions that are currently sympatric, suggesting ongoing or

recent hybridization (Fig. 3). For example, gene flow between black-tailed jackrabbits and snowshoe hares in North America ($f_b(C)$ = 19%; P = 2.04E-169), or between European brown hares and mountain hares from Eurasia ($f_b(C)$ = 18%; P = 1.73E-233; Fig. 3 and Supplementary Table S11). In general, we found decreased admixture proportions with increased genetic divergence between species, although this correlation was only significant when considering species with non-overlapping distributions (Fig. 4). Several species pairs with extant contact zones showed admixture even when genetic divergence was relatively high, such as snowshoe hares and black-tailed jackrabbits (d_{xy} = 0.97%; TMRCA ~ 4.8 Ma, Supplementary Fig. S5 and Tables S4 and S5).

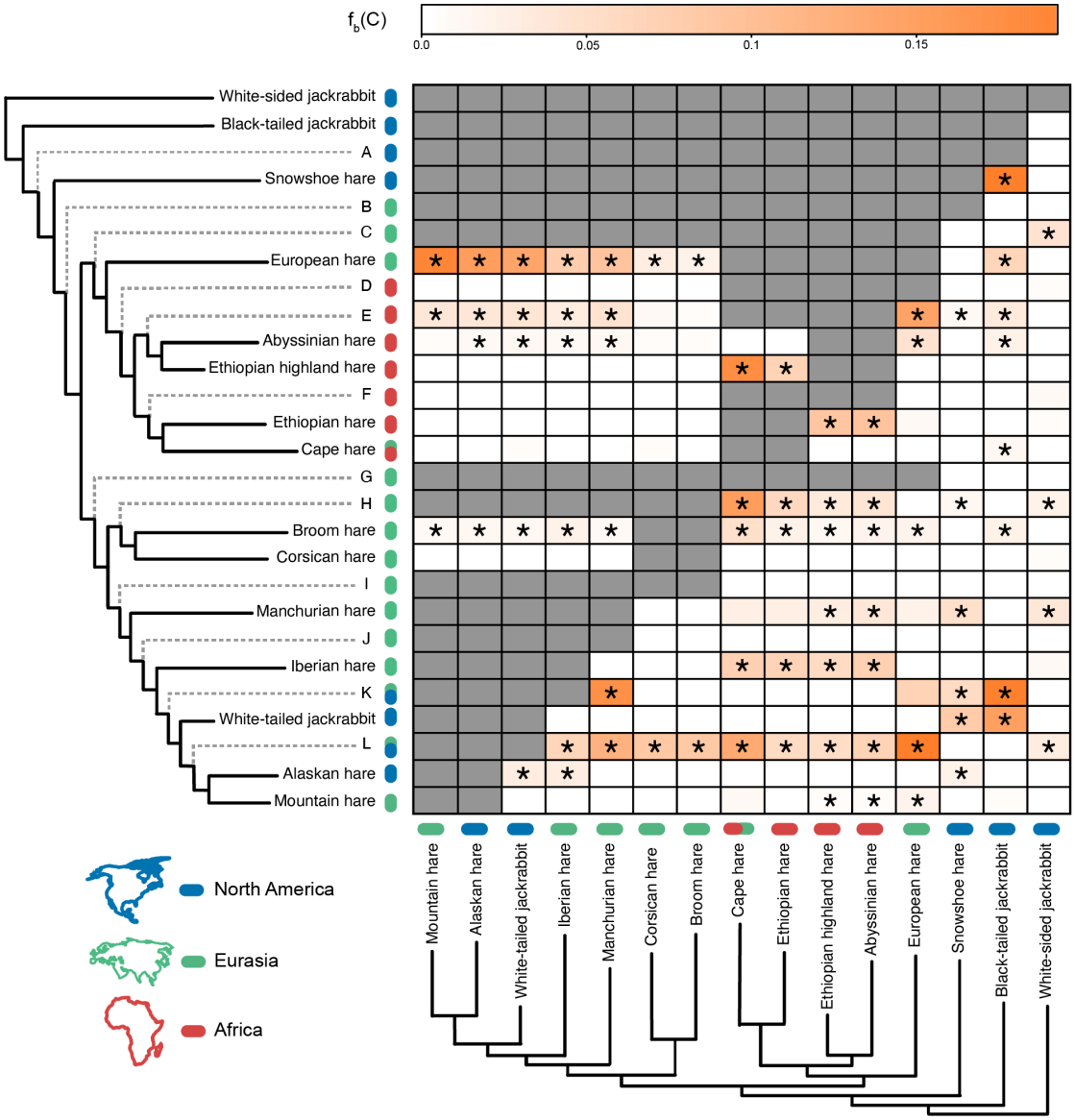

Fig. 3 – Admixture events are distributed across the hare (*Lepus* spp.) species tree. The branch-specific statistic $f_b(C)$ represents excess allele sharing between branches b (y-axis) and C (x-axis) of the species tree in Figure 1. The orange gradient represents the $f_b(C)$ score, gray represents tests not consistent with the species tree and asterisks denote block jackknifing significance at $P \leq 0.05$ (after Bonferroni correction). Tips of the tree are colored according to their current distribution (two colors represent distribution in both areas), and ancestral tips (dashed gray lines labeled with letters) are colored according to the ancestral reconstruction of distribution areas from Figure 1

470 (two colors represent equivocal inference of the two-character states). Ancestral tips are
471 labeled from A to L corresponding to labels in Supplementary Table S11.
472
473 We also found evidence for introgression between ancestral populations, which
474 has affected deeper branches of the species tree. Network and $f_b(C)$ results suggest
475 ancestral events of introgression connecting major diverged clades within Eurasia (e.g.,
476 European hares and the ancestor of the mountain hare/Alaskan hare/white-tailed
477 jackrabbit clade), African and Eurasian lineages (e.g., ancestral of all African species
478 and the Corsican and broom hare ancestral), and Eurasian and North American lineages
479 (e.g., snowshoe hares and the ancestral lineage of the mountain hare/Alaskan
480 hare/white-tailed jackrabbit; Fig. 3, 4, Supplementary Figs. S10 and S11, and Table
481 S11). Finally, we found significant allele sharing among species that currently inhabit
482 different continents, such as North American hares and species from Africa and
483 Western Europe (Fig. 3 and 4). Trans-continental introgression was also suggested by a
484 network with two reticulations and by ancestral population graph reconstruction
485 (Supplementary Figs. S10c and S11). Given the inferred split times (Supplementary Fig.
486 S5) and biogeography (Fig. 1) of this group, these results suggest that introgression
487 affected the very early branches of the *Lepus* radiation, and that the genetic legacy of
488 these gene flow events persists in the gene pool of descendant species today (Fig. 3 and
489 4).

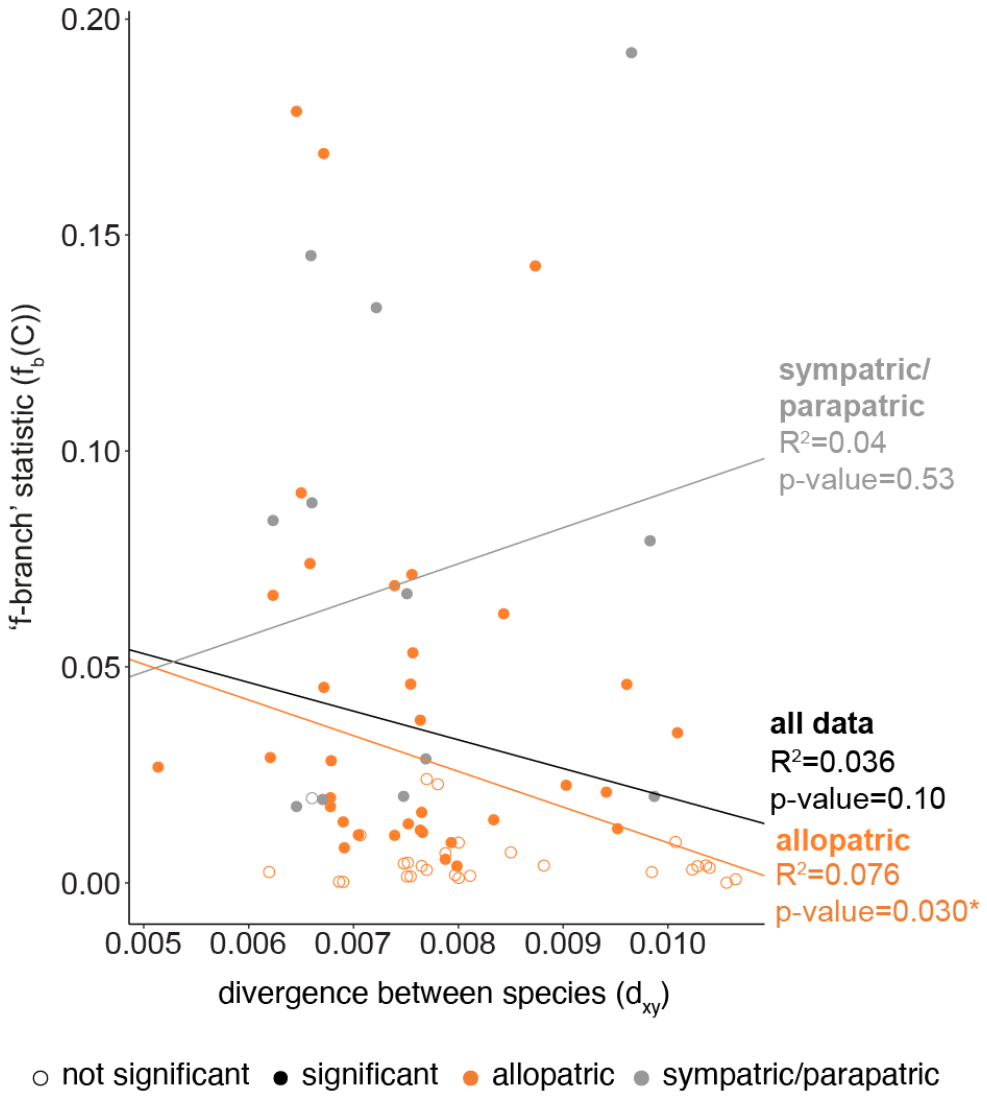

Fig. 4 – Admixture proportions decrease with genetic divergence between allopatric species. We plot *f_b(C)* values against exome-wide divergence (d_{xy}) for extant species pairs, coloring points when species have overlapping (sympatric/parapatric) or non-overlapping (allopatric) distributions. The tendency line represents a linear regression relating d_{xy} and *f_b(C)* values calculated with function *lm()* in R.

Genes affected by Ancestral Introgression

We detected ancestral introgression involving white-tailed jackrabbits, mountain hares, Alaskan hares, and snowshoe hares, which together have a circumpolar distribution across northern latitude habitats (Fig. 3 and Supplementary Fig. S10). These species

501 inhabit the strongly seasonal boreal and/or temperate environments of North America
502 and Eurasia (Smith et al. 2018), and have all evolved seasonal coat color molts from
503 summer brown to winter white to maintain cryptic coloration with the onset of seasonal
504 snow cover (Mills et al. 2018). Motivated by recent work showing that introgressive
505 hybridization has shaped local adaptation in seasonal coat color changing species (Jones
506 et al. 2018; Giska et al. 2019; Jones et al. 2020a), we next examined the contribution of
507 gene flow between the ancestor of Alaskan hare/mountain hare/white-tailed jackrabbit
508 and snowshoe hares (at least 0.98 Ma from lagomorph fossil calibrations and 0.71 Ma
509 from *Lepus* fossil calibration; Supplementary Fig. S5 and Table S5) to standing
510 variation in these species.

511 We performed fraction of admixture (f_d) scans to detect genomic regions shared
512 through ancestral introgression among these species. We detected 119 putative windows
513 of ancient introgression across all major chromosomes, highlighting the genome-wide
514 impact of ancestral introgression (Fig. 5; Supplementary Table S12). The f_d outlier
515 windows of ancestral introgression contained 54 annotated genes (Supplementary Table
516 S13). This set of genes was enriched for the gene ontology term "E-Box binding" (3 of
517 the 54 genes; Supplementary Table S14), a DNA motif found in the promoters of many
518 genes, suggesting that genomic regions affected by ancient introgression may be
519 enriched for transcription factors involved in *trans*-regulation of gene expression.
520 Among these transcription factors we found the circadian clock related gene *ARNTL2*
521 (Sasaki et al. 2009) and pigmentation related gene *TCF4* (Furumura et al. 2001; Le Pape
522 et al. 2009) (Fig. 5). In addition, the list of 54 genes includes a gene involved in brown
523 fat differentiation (*EBF2*; Rajakumari et al. 2013), and a photoreceptor-related gene
524 (*PDE6H*; Kohl et al. 2012).

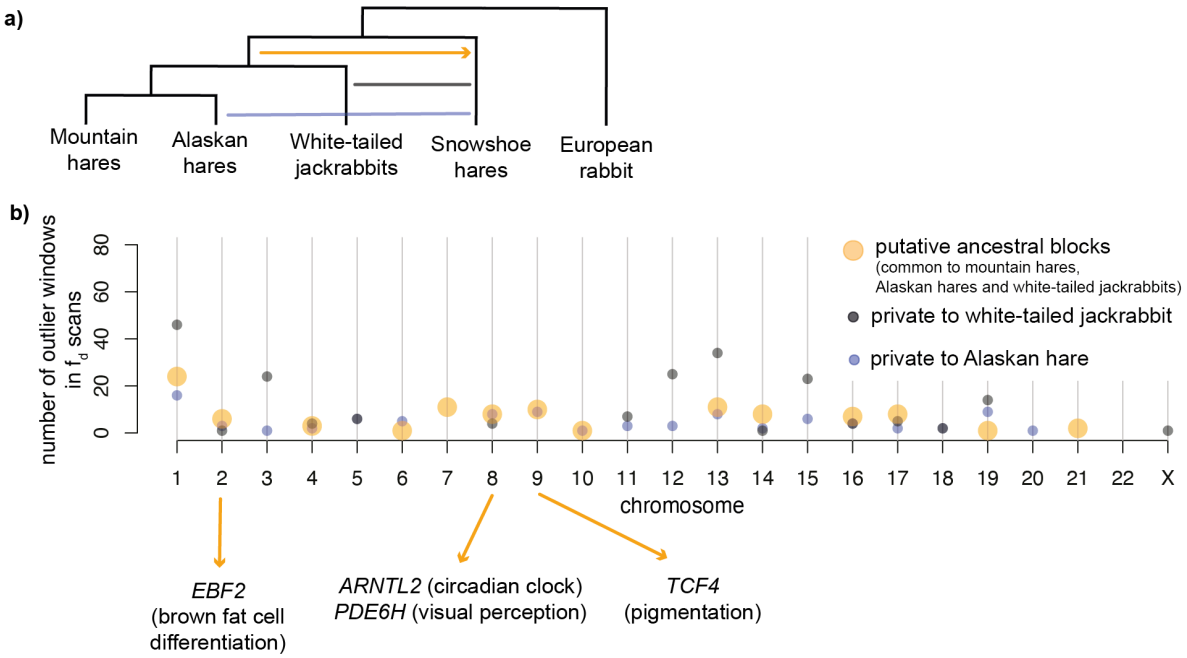

Fig. 5 – The impact of ancestral introgression on extant northern latitude species. **A)** Events of past and recent admixture inferred in this study involving snowshoe, Alaskan hares, mountain hares and white-tailed jackrabbits. The arrow indicates the direction of ancestral introgression inferred by *PhyloNet*; **B)** Genomic distribution of ancestral blocks of introgression inferred as shared outliers windows among fraction of admixture (f_d) analysis testing for admixture among snowshoe hares and each one of the three other northern latitude species (orange), and blocks private to the analysis with Alaskan hares (blue) and white-tailed jackrabbits (black). Tests were run in 50 kb genomic sliding windows, and outlier windows are in the top 0.5% of the f_d distribution.

Discussion

We used whole exome data and diverse phylogenetic analyses to tease apart signatures of stochastic lineage sorting and admixture across the evolutionary history of the *Lepus* radiation. By accounting for these sources of phylogenetic discordance, we were able to detect pervasive introgression between lineages that was layered across the evolution of this recent and rapid mammalian radiation. Below we discuss the biogeographic and

542 evolutionary implications of our analyses, focusing on the long-term impacts of
543 temporally layered hybridization in shaping patterns of shared genetic variation within
544 and among extant species.
545
546 *The Effect of Persistent Gene Flow on Phylogenetic Inference*
547 We present a resolved genome-wide phylogeny for the genus *Lepus* despite extensive
548 incomplete lineage sorting and pervasive gene flow. Although we sampled just a subset
549 of described *Lepus* species (15 of 32 species), our genome-wide experiment covered all
550 major lineages across the worldwide range of hares resulting in the most extensive
551 phylogeny of the genus to date, substantially extending previous analyses based on more
552 limited genetic sampling (Halanych et al. 1999; Melo-Ferreira et al. 2012; Ge et al. 2013;
553 Tolesa et al. 2017). A systematic evaluation of species limits and hare taxonomy is
554 beyond the scope of our work as it would require genome-wide sequencing of an
555 expanded inter and intraspecific sample. Our sampling design is however not expected to
556 bias phylogenetic relationships of the sampled species and inference of discordance
557 among deeper lineages, and may even underestimate species diversity, thus making our
558 inferences of shared variation among species conservative.
559 To estimate species relationships, we combined species tree inferences that do not
560 account for gene flow with network-based inferences that explicitly consider
561 introgression. The resulting topologies were generally consistent between methods when
562 considering up to three reticulations (Fig. 1 and Supplementary Fig. S10). However, there
563 were clear limits to this approach. For example, the alternative placement of European,
564 Corsican, and broom hares, as closer to the Eurasian or African *Lepus* clades depended
565 on the number of reticulations considered (Supplementary Fig. S10). This uncertainty
566 likely reflects long-term admixture among Eurasian and African lineages, including the

567 European hare (Fig. 3 and Supplementary Fig. S10) whose range overlaps with species
568 from both continents (Fig. 1a). Another example is the alternative sister relationship of
569 snowshoe hares and black-tailed jackrabbits in the network with no reticulation
570 (Supplementary Fig. S10), which could result from ancestral introgression between these
571 species (see below). A network with four reticulations was less concordant than results
572 assuming zero to three reticulations. While an increase number of reticulation events
573 could better represent the widespread nature of gene flow uncovered in our work,
574 allowing for more than three reticulations resulted in increased branch compression
575 suggesting that the added instances of gene flow do not contribute to resolve gene-to-
576 gene incongruences (Supplementary Fig. S10) (Yu and Nakhleh 2015; Wen et al. 2016).
577 Interestingly, we found that gene trees constructed from X-linked loci or
578 autosome-linked loci showed similar levels of discordance with the whole-genome
579 species tree (Supplementary Fig. S6). In general, the X chromosome could be expected
580 to show less phylogenetic discordance due to a typically smaller effective population
581 size (i.e., lower levels of incomplete lineage sorting assuming equal sex ratios) and a
582 tendency to accumulate hybrid incompatibilities (i.e., the large X-effect) (Fontaine et al.
583 2015; Edelman et al. 2019; Li et al. 2019). Although there is evidence for reduced X-
584 linked gene flow between some hybridizing European lineages (Seixas et al. 2018) very
585 little is known about the genetic architecture of reproductive isolation between hare
586 species. Moreover, higher gene tree/species tree concordance of loci involved in
587 reproductive isolation may not be always expected, particularly when speciation events
588 are clustered in time (Wang and Hahn 2018) as is the case in *Lepus* (Supplementary Fig.
589 S5).
590
591 *The Timing and Biogeography of the Lepus Radiation*

592 Overall, our results suggest that the *Lepus* diversification followed major climatic shifts
593 that occurred during the late Miocene, Pliocene and Pleistocene, similar to other
594 terrestrial mammals (Simpson 1947; Ge et al. 2013). We inferred that the genus
595 originated in North America between 5.83 Ma (deeper fossil calibration) and 4.05 Ma
596 (*Lepus* fossil calibration) (in general agreement with Hibbard 1963; Halanych et al.
597 1999; Melo-Ferreira et al. 2012; Ge et al. 2013). This inferred origin coincides with a
598 global cold and dry period of the late Miocene that favored the expansion of grasslands
599 worldwide (Osborne and Beerling 2006; Ge et al. 2013). The colonization of Eurasia
600 around 2.77 Ma (deeper fossil calibration) or 1.99 Ma (*Lepus* fossil calibration) is also
601 coincident with faunal exchanges between North America and Eurasia during late
602 Pliocene and Pleistocene glacial periods that connected both continents through the
603 Bering land bridge (Simpson 1947; Hopkins 1959; Cook et al. 2016). After colonizing
604 Eurasia, *Lepus* entered Africa somewhere between the divergence of the European hare
605 and the African ancestral lineage (1.78 Ma or 2.48 Ma from *Lepus* or deeper fossil
606 calibrations respectively) and the divergence of all African species (1.33 Ma or 1.85 Ma
607 from *Lepus* or deeper fossil calibrations respectively) (Supplementary Fig. S5 and Table
608 S5).

609 Our biogeographic inferences confirm a secondary colonization of North
610 America back from Eurasia likely within the last 1 Ma (Fig. 1 and Supplementary Fig.
611 S5) (Halanych et al. 1999). The Eurasia-North America exchange of fauna during
612 colder glacial periods of the Pleistocene is thought to have involved taxa adapted to
613 colder environments (Simpson 1947; Hoberg et al. 2012). Consistent with this, we find
614 that the *Lepus* re-colonization of North America involved the ancestral lineage of
615 species now adapted to northern ecosystems (i.e., mountain hares, Alaskan hares, and
616 white-tailed jackrabbits).

We note that our finding of pervasive introgression (Fig. 3, Supplementary Figs. S9, S10 and S11 and Table S11) may distort aspects of these biogeographic inferences (Leaché et al. 2014; Solís-Lemus et al. 2016; Long and Kubatko 2018; Li et al. 2019; Jiao et al. 2020). Assuming that the inferred structure of the *Lepus* phylogeny is correct, as discussed above, the general biogeographic reconstructions are probably robust. However, extensive ancestral gene flow is still likely to bias our estimates of species divergence (Leaché et al. 2014; Li et al. 2019). The lack of varied, independent, and reliable calibration points along our phylogeny hinders further evaluation of the impact of introgression on our time estimates, which therefore should be interpreted with caution.

The Legacy of Introgression during the Rapid Radiation of Hares

Extensive reticulation across the *Lepus* phylogeny suggests that lineages often hybridized when they came into contact during their worldwide expansion. Some of the inferred reticulation events overlap with known recent introgression, such as between mountain hares and European hares (Levänen et al. 2018) or between snowshoe hares and black-tailed jackrabbits (Jones et al. 2018, 2020a). However, our analysis also reveals prevailing signatures of deeper hybridization between ancestral populations, suggesting a persistent contribution of secondary introgression during the diversification of the genus. These past hybridization events have resulted in extensive shared polymorphism among extant species (Fig. 3 and Supplementary Tables S10, S11 and Figs. S9, S10 and S11), with significant admixture still detected among species with non-overlapping distributions or inhabiting different continents (Fig. 3 and Fig. 4).

Our results highlight how ancient gene flow can obscure accurate detection of contemporary hybridization. Similar to other systems (Malinsky et al. 2018; Li et al.

642 2019; Edelman et al. 2019), we estimated exceedingly high levels of introgression based
643 on D-statistics (e.g., 88% of D_{min} values across all possible species trios were
644 significant), but much less reticulation when we took the phylogeny into account (e.g.,
645 33% of f-branch statistics were significant). These findings suggest that some signatures
646 of introgression between pairs of species may actually result from earlier hybridization
647 between ancestral lineages. Thus, phylogenetic correlation causes non-independence of
648 summary-statistics and can thus lead to false positive inferences of gene flow (Eaton et
649 al. 2015; Malinsky et al. 2018; Li et al. 2019). Given these results, signatures of
650 hybridization among closely related species should be interpreted in the context of
651 broader phylogenetic relationships whenever possible.

652 We also detected some discrepancies between the magnitude of gene flow
653 inferred here and in previous works, which underscores the challenges of quantifying
654 introgression across a reticulating radiation. For instance, we inferred substantial overall
655 admixture proportions between black-tailed jackrabbits and snowshoe hares ($f_b(C)$ =
656 19%, Fig. 3 and Supplementary Table S11). These estimates are one order of magnitude
657 higher than recent studies suggesting that ~2-3% of genomic variation in the Pacific
658 Northwest snowshoe hare populations descends from a pulse of gene flow from black-
659 tailed jackrabbits in the last ~10,000 generations (Jones et al. 2018, 2020a). Ancient
660 introgression persisting in all snowshoe hare populations could reconcile this
661 discrepancy. Indeed, we recovered admixture in the same order of magnitude (f_{hom} ~3%)
662 when we infer admixture proportions among different snowshoe hare populations and
663 black-tailed jackrabbits (Supplementary Table S15), which would then reflect recent
664 and geographically localized introgression. However, our quantitative estimate of
665 overall admixture proportions between these species (19%) also depends on the accurate
666 reconstruction of the species tree, which in this instance involves a short internal branch

667 that is not fully supported across methods, and a species (snowshoe hare) that has been
668 involved in multiple instances of introgression with different hare lineages (Fig. 3, 5
669 and Supplementary Table S11 and Fig. S10).

670 Introgression between species is often limited by purifying selection against
671 divergent alleles that are deleterious in hybrids (Schumer et al. 2018; Edelman et al.
672 2019), which agrees with the predominantly negative consequences of hybridization
673 (Mayr 1963). Nonetheless, hybridization is also expected to produce novel allelic
674 combinations that increase phenotypic variation (Grant and Grant 2019; Marques et al.
675 2019). If coincident with ecological opportunity, introgressed variation could broadly
676 facilitate adaptation (Grant and Grant 2019; Taylor and Larson 2019). Recent work has
677 shown at least two instances where introgression between *Lepus* species has driven
678 local adaptation (Jones et al. 2018; Giska et al. 2019), and standing variation from
679 introgression may have contributed even more generally to adaptation during the
680 radiation. We found here that allelic combinations from ancient hybridization can be
681 carried through several speciation events (Fig. 3 and 4), persisting in the gene pool of
682 consecutive species due to the rapid succession of speciation events. Much of the large
683 reservoir of shared variation may reflect stochastic sorting of neutral variation, while
684 some could be maintained by positive selection (Guerrero and Hahn 2017), facilitating
685 colonization of the diverse habitats currently inhabited by hare species, from desert to
686 arctic environments (Ge et al. 2013; Smith et al. 2018).

687 In this respect, introgression between the ancestor of mountain hares/Alaskan
688 hares/white-tailed jackrabbits and snowshoe hares (or an ancestral lineage) is
689 particularly intriguing. These four species have adapted to highly seasonal environments
690 through striking forms of phenotypic plasticity (e.g., seasonal coat color change; Mills
691 et al. 2013; Zimova et al. 2018) that have been at least partially shaped by adaptive

692 introgression at the *Agouti* pigmentation gene from non-color changing species (*ASIP*;
693 Jones et al. 2018; Giska et al. 2019). Here we estimated that a pulse of ancient
694 introgression occurred at least 0.71 Ma (*Lepus* fossil calibration; Supplementary Fig.
695 S5) and affected genomic regions containing genes associated with circadian rhythm
696 regulation (*ARNTL2*; Sasaki et al. 2009), pigmentation (*TCF4*; Furumura et al. 2001; Le
697 Pape et al. 2009), thermoregulation (*EBF2*; Rajakumari et al. 2013) and visual
698 perception (*PDE6H*; Kohl et al. 2012). While *ASIP* would also be a likely candidate for
699 adaptive introgression between these lineages (Jones et al. 2018), our exome sequencing
700 coverage of this region was too sparse for detailed window-based analysis.

701 The functions of these introgressed genes overlap with common physiological
702 adaptations of northern latitude animals to seasonal conditions, such as higher metabolic
703 rates, regulation of body temperature and non-shivering thermogenesis (Hart et al. 1965;
704 Feist and Rosenmann 1975; Rogowitz 1990; Pyörnilä et al. 2008; Sheriff et al. 2009),
705 seasonal camouflage (Grange 1932; Hewson 1958; Hansen and Bear 1963; Mills et al.
706 2018; Zimova et al. 2018), and visual acuity in response to dim winter light in northern
707 latitudes (Stokkan et al. 2013). The functional relevance of these candidates to local
708 adaptation must await further testing. Substantial introgression along the rapid
709 diversification of a group of organisms, as we describe here, may bolster genetic
710 variation within species and have a greater role in local adaptation than previously
711 anticipated (Grant and Grant 2019; Taylor and Larson 2019). However, we also cannot
712 exclude the possibility that some of these shared variants have been maintained by long-
713 term balancing selection rather than secondary introgression (Supplementary Fig. S13;
714 Smith and Kronforst 2013; Liu et al. 2015; Guerrero and Hahn 2017). Regardless of
715 origin, the *Lepus* radiation provides an intriguing system by which to test the long-term
716 evolutionary importance of shared genetic variation across a rapid radiation.

DATA AVAILABILITY

Raw sequence reads were deposited at the Sequence Read Archive (SRA) under accession numbers SRR12020579 to SRR12020510 and BioProject PRJNA639005. Other data will be made available from the Dryad Digital Repository with link http://dx.doi.org/10.5061/dryad.[NNNN]. The pipeline and custom scripts used for this study are available at https://github.com/evochange.

ACKNOWLEDGEMENTS

We thank Janet Rachlow, Gloria Portales, Armando Geraldes, José Carlos Brito, Jérôme Letty, Conrad Matthee, Alexei Kryukov, Ettore Randi, Christian Gortazar, Rafael Villafuerte, Fernando Ballesteros, Klaus Hackländer and Zbyszek Boratynski for assistance with sample collection. The Alaskan hare samples used in this work were generously provided by the University of Alaska Museum (voucher codes UAM42143 and UAM45545). We thank Fernando Seixas, Tiago Antão, Hannes Svardal, Nathaniel Edelman, the EVOCHANGE lab, the Good lab, and the UNVEIL network for helpful discussions on the generation and analysis of data. Funding and support for this research was provided by Fundação para a Ciência e a Tecnologia (FCT) (project grant "CHANGE" – PTDC/BIA-EVF/1624/2014, Portuguese National Funds) and the National Science Foundation (NSF) (EPSCoR OIA-1736249 and DEB-1907022 grant). MSF was supported by POPH-QREN funds from ESF and Portuguese MCTES/FCT (PD/BD/108131/2015 PhD grant in the scope of BIODIV PhD programme at Faculty of Sciences, University of Porto), Portuguese National Funds through FCT (PTDC/BIA-EVF/1624/2014), and by NSF (OIA-1736249). MRJ was supported by an NSF Graduate Research Fellowship (DGE-1313190). JM-F was

742 supported by an FCT CEEC contract (CEECIND/00372/2018). Instrumentation,
743 laboratory, and computational support was provided by CIBIO NEWGEN sequencing
744 platform, supported by European Union's Seventh Framework Program for research,
745 technological development and demonstration under grant agreement no. 286431, by
746 the University of Montana Genomics Core, supported by a grant from the M.J. Murdock
747 Charitable Trust. A grant from the Eunice Kennedy Shriver National Institute of Child
748 Health and Human Development (R01HD073439) supported the development of exome
749 capture protocols that were utilized in the current study. Additional support was
750 obtained from the Laboratoire International Associé (LIA) "Biodiversity and Evolution"
751 funded by InEE (CNRS, France) and FCT (Portugal), COMPETE2020,
752 PORTUGAL2020, and ERDF (POCI-01-0145-FEDER-022184), and from Portugal-
753 United States of America Research Networks Program funds from Fundação Luso-
754 Americana para o Desenvolvimento (FLAD) to PCA and MSF.

755

756 **REFERENCES**

757 Alves P.C., Melo-Ferreira J., Branco M., Suchentrunk F., Ferrand N., Harris D.J. 2008.
758 Evidence for genetic similarity of two allopatric European hares (*Lepus corsicanus*
759 and *L. castroviejoi*) inferred from nuclear DNA sequences. Mol. Phylogenet. Evol.
760 46:1191–7.

761 Árnason Ú., Lammers F., Kumar V., Nilsson M.A., Janke A. 2018. Whole-genome
762 sequencing of the blue whale and other rorquals finds signatures for introgressive
763 gene flow. Sci. Adv. 4.

764 Van der Auwera G.A., Carneiro M.O., Hartl C., Poplin R., del Angel G., Levy-
765 Moonshine A., Jordan T., Shakir K., Roazen D., Thibault J., Banks E., Garimella
766 K. V, Altshuler D., Gabriel S., DePristo M.A. 2013. From fastQ data to high-

767 confidence variant calls: The genome analysis toolkit best practices pipeline. Curr.
768 Protoc. Bioinforma. 11.
769 Barlow A., Cahill J.A., Hartmann S., Theunert C., Xenikoudakis G., Fortes G.G.,
770 Paijmans J.L.A., Rabeder G., Frischauf C., Grandal-d'Anglade A., García-Vázquez
771 A., Murtskhvaladze M., Saarma U., Anijalg P., Skrbinšek T., Bertorelle G.,
772 Gasparian B., Bar-Oz G., Pinhasi R., Slatkin M., Dalén L., Shapiro B., Hofreiter
773 M. 2018. Partial genomic survival of cave bears in living brown bears. Nat. Ecol.
774 Evol. 2:1563–1570.
775 Barth J.M.I., Gubili C., Matschiner M., Tørresen O.K., Watanabe S., Egger B., Han
776 Y.S., Feunteun E., Sommaruga R., Jehle R., Schabetsberger R. 2020. Stable
777 species boundaries despite ten million years of hybridization in tropical eels. Nat.
778 Commun. 11:1–13.
779 Bennett D.J., Sutton M.D., Turvey S.T. 2017. Treeman: An R package for efficient and
780 intuitive manipulation of phylogenetic trees. BMC Res. Notes. 10:30.
781 Borowiec M.L. 2016. AMAS: A fast tool for alignment manipulation and computing of
782 summary statistics. PeerJ. 2016:e1660.
783 Carneiro M., Rubin C.J., Palma F. Di, Albert F.W., Alföldi J., Barrio A.M., Pielberg G.,
784 Rafati N., Sayyab S., Turner-Maier J., Younis S., Afonso S., Aken B., Alves J.M.,
785 Barrell D., Bolet G., Boucher S., Burbano H.A., Campos R., Chang J.L.,
786 Duranthon V., Fontanesi L., Garreau H., Heiman D., Johnson J., Mage R.G., Peng
787 Z., Queney G., Rogel-Gaillard C., Ruffier M., Searle S., Villafuerte R., Xiong A.,
788 Young S., Forsberg-Nilsson K., Good J.M., Lander E.S., Ferrand N., Lindblad-Toh
789 K., Andersson L. 2014. Rabbit genome analysis reveals a polygenic basis for
790 phenotypic change during domestication. Science. 345:1074–1079.
791 Chifman J., Kubatko L. 2014. Quartet inference from SNP data under the coalescent

792 model. Bioinformatics. 30:3317–3324.

793 Cook J.A., Galbreath K.E., Bell K.C., Campbell M.L., Carrière S., Colella J.P., Dawson
794 N.G., Dunnum J.L., Eckerlin R.P., Fedorov V., Greiman S.E., Haas G.M.,
795 Haukisalmi V., Henttonen H., Hope A.G., Jackson D., Jung T.S., Koehler A. V,
796 Kinsella J.M., Krejsa D., Kutz S.J., Liphardt S., MacDonald S.O., Malaney J.L.,
797 Makarikov A., Martin J., McLean B.S., Mulders R., Nyamsuren B., Talbot S.L.,
798 Tkach V. V, Tsvetkova A., Toman H.M., Waltari E.C., Whitman J.S., Hoberg E.P.,
799 Cook J., Bell K., Colella J., Jackson D., Krejsa D., Liphardt S., McLean B.,
800 Galbreath K., Haas G., Toman H., Campbell M., Dunnum J., MacDonald S.,
801 Carrière S., Mulders R., Dawson N., Fedorov V., Greiman S., Jung T., Koehler A.,
802 Kinsella J., Kutz S., Malaney J., Makarikov A., Martin J., Nyamsuren B., Waltari
803 Aaron E., Hoberg Animal E. 2016. The Beringian Coevolution Project: holistic
804 collections of mammals and associated parasites reveal novel perspectives on
805 evolutionary and environmental change in the North. Arct. Sci. 3:585–617.

806 Degnan J.H. 2018. Modeling Hybridization Under the Network Multispecies
807 Coalescent. Syst. Biol. 67:786–799.

808 Durinck S., Moreau Y., Kasprzyk A., Davis S., De Moor B., Brazma A., Huber W.
809 2005. BioMart and Bioconductor: a powerful link between biological databases
810 and microarray data analysis. Bioinformatics. 21:3439–3440.

811 Durinck S., Spellman P.T., Birney E., Huber W. 2009. Mapping identifiers for the
812 integration of genomic datasets with the R/ Bioconductor package biomaRt. Nat.
813 Protoc. 4:1184–1191.

814 Eaton D.A.R., Hipp A.L., González-Rodríguez A., Cavender-Bares J. 2015. Historical
815 introgression among the American live oaks and the comparative nature of tests for
816 introgression. Evolution. 69:2587–2601.

Edelman N.B., Frandsen P.B., Miyagi M., Clavijo B., Davey J., Dikow R.B., García-Accinelli G., Van Belleghem S.M., Patterson N., Neafsey D.E., Challis R., Kumar S., Moreira G.R.P., Salazar C., Chouteau M., Counterman B.A., Papa R., Blaxter M., Reed R.D., Dasmahapatra K.K., Kronforst M., Joron M., Jiggins C.D., Owen McMillan W., Palma F. Di, Blumberg A.J., Wakeley J., Jaffe D., Mallet J. 2019. Genomic architecture and introgression shape a butterfly radiation. Science. 366:594–599.

Feist D.D., Rosenmann M. 1975. Seasonal sympatho-adrenal and metabolic responses to cold in the Alaskan snowshoe hare (*Lepus americanus macfarlani*). Comp. Biochem. Physiol. Part A Physiol. 51:449–455.

Fontaine M.C., Pease J.B., Steele A., Waterhouse R.M., Neafsey D.E., Sharakhov I. V, Jiang X., Hall A.B., Catteruccia F., Kakani E., Mitchell S.N., Wu Y.-C., Smith H.A., Love R.R., Lawniczak M.K., Slotman M.A., Emrich S.J., Hahn M.W., Besansky N.J. 2015. Extensive introgression in a malaria vector species complex revealed by phylogenomics. Science. 347:1258522–1258522.

Furumura M., Potterf S.B., Toyofuku K., Matsunaga J., Muller J., Hearing V.J. 2001. Involvement of ITF2 in the transcriptional regulation of melanogenic genes. J. Biol. Chem. 276:28147–54.

Ge D., Wen Z., Xia L., Zhang Z., Erbajeva M., Huang C., Yang Q. 2013. Evolutionary History of Lagomorphs in Response to Global Environmental Change. PLoS One. 8:e59668.

Giska I., Farelo L., Pimenta J., Seixas F.A., Ferreira M.S., Marques J.P., Miranda I., Letty J., Jenny H., Hackländer K., Magnussen E., Melo-Ferreira J. 2019. Introgression drives repeated evolution of winter coat color polymorphism in hares. Proc. Natl. Acad. Sci. 116:24150–24156.

Gittelman R.M., Schraiber J.G., Vernot B., Mikacenic C., Wurfel M.M., Akey J.M. 2016. Archaic Hominin Admixture Facilitated Adaptation to Out-of-Africa Environments. Curr. Biol. 26:1–8.

Grange W.B. 1932. The Pelages and Color Changes of the Snowshoe Hare, *Lepus americanus phaeonotus*, Allen. J. Mammal. 13:99.

Grant P.R., Grant B.R. 2019. Hybridization increases population variation during adaptive radiation. Proc. Natl. Acad. Sci. 116:23216–23224.

Green R.E., Krause J., Briggs A.W., Maricic T., Stenzel U., Kircher M., Patterson N., Li H., Zhai W., Fritz M.H.-Y., Hansen N.F., Durand E.Y., Malaspinas A.-S., Jensen J.D., Marques-Bonet T., Alkan C., Prüfer K., Meyer M., Burbano H.A., Good J.M., Schultz R., Aximu-Petri A., Butthof A., Höber B., Höffner B., Siegemund M., Weihmann A., Nusbaum C., Lander E.S., Russ C., Novod N., Affourtit J., Egholm M., Verna C., Rudan P., Brajkovic D., Kucan Ž., Gušic I., Doronichev V.B., Golovanova L. V, Lalueza-Fox C., de la Rasilla M., Fortea J., Rosas A., Schmitz R.W., Johnson P.L.F., Eichler E.E., Falush D., Birney E., Mullikin J.C., Slatkin M., Nielsen R., Kelso J., Lachmann M., Reich D., Pääbo S. 2010. A draft sequence of the Neandertal genome. Science. 328:710–722.

Guerrero R.F., Hahn M.W. 2017. Speciation as a sieve for ancestral polymorphism. Mol. Ecol. 26:5362–5368.

Halanych K.M., Demboski J.R., van Vuuren B.J., Klein D.R., Cook J. a. 1999. Cytochrome b phylogeny of North American hares and jackrabbits (*Lepus*, Lagomorpha) and the effects of saturation in outgroup taxa. Mol. Phylogenet. Evol. 11:213–221.

Hansen R.M., Bear G.D. 1963. Winter coats of white-tailed jackrabbits in southwestern Colorado. J. Mammology. 44:420–422.

867 Hart J.S., Pohl H., Tener J.S. 1965. Seasonal acclimatization in varying hare (*Lepus*
868 *americanus*). Can. J. Zool. 43:731–744.
869 Hewson R. 1958. Moults and winter whitening in the mountain hare *Lepus timidus*
870 *scoticus*, Hilzheimer. Proc. Zool. Soc. London. 131:99–108.
871 Hibbard C. 1963. The Origin of the P 3 Pattern of *Sylvilagus*, *Caprolagus*, *Oryctolagus*
872 and *Lepus*. J. Mammal. 44:1–15.
873 Hoberg E.P., Galbreath K.E., Cook J.A., Kutz S.J., Polley L. 2012. Northern Host-
874 Parasite Assemblages. History and Biogeography on the Borderlands of Episodic
875 Climate and Environmental Transition. Advances in Parasitology. Academic Press.
876 p. 1–97.
877 Hopkins D.M. 1959. Cenozoic history of the Bering land bridge. Science. 129:1519–
878 1528.
879 Huson D.H., Bryant D. 2006. Application of phylogenetic networks in evolutionary
880 studies. Mol. Biol. Evol. 23:254–267.
881 Inoue J., Donoghue P.C.J., Yang Z. 2010. The Impact of the Representation of Fossil
882 Calibrations on Bayesian Estimation of Species Divergence Times. Syst. Biol.
883 59:74–89.
884 Jiao X., Flouri T., Rannala B., Yang A.Z. 2020. The Impact of Cross-Species Gene
885 Flow on Species Tree Estimation. Syst. Biol. 0:1–18.
886 Jones M.R., Mills L.S., Alves P.C., Callahan C.M., Alves J.M., Lafferty D.J.R., Jiggins
887 F.M., Jensen J.D., Melo-Ferreira J., Good J.M. 2018. Adaptive introgression
888 underlies polymorphic seasonal camouflage in snowshoe hares. Science.
889 360:1355–1358.
890 Jones M.R., Mills L.S., Jensen J.D., Good J.M. 2020a. The origin and spread of locally
891 adaptive seasonal camouflage in snowshoe hares. Am. Nat.

https://doi.org/10.1086/710022

Jones M.R., Mills L.S., Jensen J.D., Good J.M. 2020b. Convergent evolution of seasonal camouflage in response to reduced snow cover across the snowshoe hare range. Evolution. Early View. https://doi.org/10.1111/evo.13976

Kinoshita G., Nunome M., Kryukov A.P., Kartavtseva I. V., Han S.-H., Yamada F., Suzuki H. 2019. Contrasting phylogeographic histories between the continent and islands of East Asia: Massive mitochondrial introgression and long-term isolation of hares (Lagomorpha: *Lepus*). Mol. Phylogenet. Evol. 136:65–75.

Kohl S., Coppieters F., Meire F., Schaich S., Roosing S., Brennenstuhl C., Bolz S., van Genderen M.M., Riemslag F.C.C., Lukowski R., den Hollander A.I., Cremers F.P.M., De Baere E., Hoyng C.B., Wissinger B. 2012. A Nonsense Mutation in *PDE6H* Causes Autosomal-Recessive Incomplete Achromatopsia. Am. J. Hum. Genet. 91:527–532.

Kozak K.M., McMillan O., Joron M., Jiggins C.D. 2018. Genome-wide admixture is common across the *Heliconius* radiation. bioRxiv. https://doi.org/10.1101/414201

Lado S., Alves P.C., Islam M.Z., Brito J.C., Melo-Ferreira J. 2019. The evolutionary history of the Cape hare (*Lepus capensis sensu lato*): insights for systematics and biogeography. Heredity. 123:634–646.

Lamichhaney S., Berglund J., Almén M.S., Maqbool K., Grabherr M., Martinez-Barrio A., Promerová M., Rubin C.-J., Wang C., Zamani N., Grant B.R., Grant P.R., Webster M.T., Andersson L. 2015. Evolution of Darwin's finches and their beaks revealed by genome sequencing. Nature. 518:371–375.

Leaché A.D., Harris R.B., Rannala B., Yang Z. 2014. The Influence of Gene Flow on Species Tree Estimation: A Simulation Study. Syst. Biol. 63:17–30.

Levänen R., Thulin C.-G., Spong G., Pohjoismäki J.L.O. 2018. Widespread

917 introgression of mountain hare genes into Fennoscandian brown hare populations.
918 PLoS One. 13:e0191790.
919 Lewis P.O. 2001. A Likelihood Approach to Estimating Phylogeny from Discrete
920 Morphological Character Data. Syst. Biol. 50:913–925.
921 Li G., Figueiró H. V, Eizirik E., Murphy W.J., Yoder A. 2019. Recombination-Aware
922 Phylogenomics Reveals the Structured Genomic Landscape of Hybridizing Cat
923 Species. Mol. Biol. Evol. 36:2111–2126.
924 Li H. 2011. A statistical framework for SNP calling, mutation discovery, association
925 mapping and population genetical parameter estimation from sequencing data.
926 Bioinformatics. 27:2987–2993.
927 Li H. 2013. Aligning sequence reads, clone sequences and assembly contigs with BWA-
928 MEM. arXiv Prepr. arXiv:1303.
929 Li H., Handsaker B., Wysoker A., Fennell T., Ruan J., Homer N., Marth G., Abecasis
930 G., Durbin R. 2009. The Sequence Alignment/Map format and SAMtools.
931 Bioinformatics. 25:2078–9.
932 Liu J., Yu L., Arnold M.L., Wu C.-H., Wu S.-F., Lu X., Zhang Y.-P. 2011. Reticulate
933 evolution: frequent introgressive hybridization among chinese hares (genus *Lepus*)
934 revealed by analyses of multiple mitochondrial and nuclear DNA loci. BMC Evol.
935 Biol. 11:223.
936 Liu K.J., Steinberg E., Yozzo A., Song Y., Kohn M.H., Nakhleh L. 2015. Interspecific
937 introgressive origin of genomic diversity in the house mouse. 112:196–201.
938 Long C., Kubatko L. 2018. The Effect of Gene Flow on Coalescent-based Species-Tree
939 Inference. Syst. Biol. 67:770–785.
940 Lopez-Martinez N. 2008. The lagomorph fossil record and the origin of the European
941 rabbit. In: Alves P.C., Ferrand N., Häcklander K., editors. Lagomorph Biology:

Evolution, Ecology and Conservation. Verlag Berlin Heidelberg: Springer. p. 27–46.

Maddison W.P., Maddison D.R. 2018. Mesquite: a modular system for evolutionary analysis. Version 3.51.

Malinsky M., Svardal H., Tyers A.M., Miska E.A., Genner M.J., Turner G.F., Durbin R. 2018. Whole-genome sequences of Malawi cichlids reveal multiple radiations interconnected by gene flow. Nat. Ecol. Evol. 2:1940–1955.

Marques D.A., Meier J.I., Seehausen O. 2019. A Combinatorial View on Speciation and Adaptive Radiation. Trends Ecol. Evol. 34:531–544.

Martin S.H., Davey J.W., Jiggins C.D. 2015. Evaluating the use of ABBA-BABA statistics to locate introgressed loci. Mol. Biol. Evol. 32:244–257.

Matthee C., Van Vuuren B., Bell D., Robinson T. 2004. A Molecular Supermatrix of the Rabbits and Hares (Leporidae) Allows for the Identification of Five Intercontinental Exchanges During the Miocene. Syst. Biol. 53:433–447.

Mayr E. 1963. Animal species and evolution. Eugen. Rev. 55:226–228.

Meier J.I., Marques D.A., Mwaiko S., Wagner C.E., Excoffier L., Seehausen O. 2017. Ancient hybridization fuels rapid cichlid fish adaptive radiations. Nat. Commun. 8:14363.

Melo-Ferreira J., Alves P.C. 2018. Systematics of lagomorphs. In: Smith A., Alves P.C., Häcklander K., editors. Lagomorphs: pikas, rabbits, and hares of the World. John Hopkins University Press. p. 9–12.

Melo-Ferreira J., Boursot P., Carneiro M., Esteves P.J., Farelo L., Alves P.C. 2012. Recurrent introgression of mitochondrial DNA among hares (*Lepus* spp.) revealed by species-tree inference and coalescent simulations. Syst. Biol. 61:367–381.

Melo-Ferreira J., Seixas F.A., Cheng E., Mills L.S., Alves P.C. 2014. The hidden

967 history of the snowshoe hare, *Lepus americanus*: extensive mitochondrial DNA
968 introgression inferred from multilocus genetic variation. Mol. Ecol.:4617–4630.
969 Meyer M., Kircher M. 2010. Illumina Sequencing Library Preparation for Highly
970 Multiplexed Target Capture and Sequencing. Cold Spring Harb. Protoc. 2010.
971 Mills L.S., Bragina E., Kumar A. V., Zimova M., Feltner J., Davis B., Lafferty D.,
972 Häcklander K., Alves P.C., Good J.M., Melo-Ferreira J., Abramov A., Lopatina
973 N., Fay K. 2018. Winter coat color polymorphisms identify global hotspots for
974 evolutionary rescue from climate change. Science. 359:1033–1036.
975 Mills L.S., Zimova M., Oyler J., Running S., Abatzoglou J.T., Lukacs P.M. 2013.
976 Camouflage mismatch in seasonal coat color due to decreased snow duration. Proc.
977 Natl. Acad. Sci. U. S. A. 110:7360–7365.
978 Osborne C.P., Beerling D.J. 2006. Nature's green revolution: the remarkable
979 evolutionary rise of C 4 plants. Philos. Trans. R. Soc. B Biol. Sci. 361:173–194.
980 Pagel M. 1999. The maximum likelihood approach to reconstructing ancestral character
981 states of discrete characters on phylogenies. Syst. Biol. 48:612–622.
982 Le Pape E., Passeron T., Giubellino A., Valencia J.C., Wolber R., Hearing V.J. 2009.
983 Microarray analysis sheds light on the dedifferentiating role of agouti signal
984 protein in murine melanocytes via the Mc1r. Proc. Natl. Acad. Sci. U. S. A.
985 106:1802–1807.
986 Paradis E., Claude J., Strimmer K. 2004. APE: Analyses of Phylogenetics and
987 Evolution in R language. Bioinformatics. 20:289–290.
988 Pease J.B., Hahn M.W. 2015. Detection and Polarization of Introgression in a Five-
989 Taxon Phylogeny. Syst. Biol. 64:651–662.
990 Pickrell J.K., Pritchard J.K. 2012. Inference of Population Splits and Mixtures from
991 Genome-Wide Allele Frequency Data. PLoS Genet. 8:e1002967.

992 Pyörnilä A., Putaala A., Hissa R., Sulkava S. 2008. Adaptations to environment in the
993 mountain hare (*Lepus timidus*): thermal physiology and histochemical properties of
994 locomotory muscles. Can. J. Zool. 70:1325–1330.
995 Rajakumari S., Wu J., Ishibashi J., Lim H.-W., Giang A.-H., Won K.-J., Reed R.R.,
996 Seale P. 2013. EBF2 Determines and Maintains Brown Adipocyte Identity. Cell
997 Metab. 17:562–574.
998 Raudvere U., Kolberg L., Kuzmin I., Arak T., Adler P., Peterson H., Vilo J. 2019.
999 g:Profiler: a web server for functional enrichment analysis and conversions of gene
1000 lists (2019 update). Nucleic Acids Res. 47:191–198.
1001 Reich D., Thangaraj K., Patterson N., Price A.L., Singh L. 2009. Reconstructing Indian
1002 population history. Nature. 461:489–494.
1003 dos Reis M., Yang Z. 2011. Approximate Likelihood Calculation on a Phylogeny for
1004 Bayesian Estimation of Divergence Times. Mol. Biol. Evol. 28:2161–2172.
1005 dos Reis M., Yang Z. 2019. Bayesian Molecular Clock Dating Using Genome-Scale
1006 Datasets. In: Anisimova M., editor. Evolutionary Genomics. New York, NY:
1007 Springer New York. p. 309–330.
1008 Rogowitz G.L. 1990. Seasonal Energetics of the White-Tailed Jackrabbit (*Lepus*
1009 *townsendii*). J. Mammal. 71:277–285.
1010 Salichos L., Stamatakis A., Rokas A. 2014. Novel information theory-based measures
1011 for quantifying incongruence among phylogenetic trees. Mol. Biol. Evol. 31:1261–
1012 1271.
1013 Sambrook E., Fritsch F., Maniatis T. 1989. Molecular cloning. Cold Spring Harbour,
1014 NY: Cold Spring Harbour Press.
1015 Sarver B.A.J., Keeble S., Cosart T., Tucker P.K., Dean M.D., Good J.M. 2017.
1016 Phylogenomic Insights into Mouse Evolution Using a Pseudoreference Approach.

1017 Genome Biol. Evol. 9:726–739.

1018 Sasaki M., Yoshitane H., Du N.-H., Okano T., Fukada Y. 2009. Preferential Inhibition
1019 of BMAL2-CLOCK Activity by PER2 Reemphasizes Its Negative Role and a
1020 Positive Role of BMAL2 in the Circadian Transcription. J. Biol. Chem.
1021 284:25149–25159.

1022 Sayyari E., Whitfield J.B., Mirarab S. 2018. DiscoVista: Interpretable visualizations of
1023 gene tree discordance. Mol. Phylogenet. Evol. 122:110–115.

1024 Schliep K.P. 2011. phangorn: phylogenetic analysis in R. Bioinform. 27:592–593.

1025 Schluter D., Price T., Mooers A.O., Ludwig D. 1997. Likelihood of ancestral states in
1026 adaptive radiation. Evolution. 51:1699–1711.

1027 Schumer M., Xu C., Powell D.L., Durvasula A., Skov L., Holland C., Blazier J.C.,
1028 Sankararaman S., Andolfatto P., Rosenthal G.G., Przeworski M. 2018. Natural
1029 selection interacts with recombination to shape the evolution of hybrid genomes.
1030 Science. 360:656–660.

1031 Seixas F.A., Boursot P., Melo-Ferreira J. 2018. The genomic impact of historical
1032 hybridization with massive mitochondrial DNA introgression. Genome Biol.
1033 19:91.

1034 Sheriff M.J., Kuchel L., Boutin S., Humphries M.M. 2009. Seasonal Metabolic
1035 Acclimatization in a Northern Population of Free-Ranging Snowshoe Hares, *Lepus*
1036 *americanus*. J. Mammal. 90:761–767.

1037 Simpson G.G. 1947. Holarctic mammalian faunas and continental relationships during
1038 the cenozoic. Bull. Geol. Soc. Am. 58:613–688.

1039 Smith A.T., Johnston C.H., Alves P.C., Häcklander K. 2018. Lagomorphs: Pikas,
1040 Rabbits and Hares of the World. Baltimore: Johns Hopkins University Press.

1041 Smith J., Kronforst M.R. 2013. Do *Heliconius* butterfly species exchange mimicry

alleles? Biol. Lett. 9:20130503–20130503.

Solís-Lemus C., Bastide P., Ané C. 2017. PhyloNetworks: A Package for Phylogenetic Networks. Mol. Biol. Evol. 34:3292–3298.

Solís-Lemus C., Yang M., Ané C. 2016. Inconsistency of Species Tree Methods under Gene Flow. Syst. Biol. 65:843–851.

Stamatakis A. 2018. RAxML version 8: a tool for phylogenetic analysis and post-analysis of large phylogenies. Bioinformatics. 30:1312–1313.

Stokkan K.-A., Folkow L., Dukes J., Neveu M., Hogg C., Siefken S., Dakin S.C., Jeffery G. 2013. Shifting mirrors: adaptive changes in retinal reflections to winter darkness in Arctic reindeer. Proc. R. Soc. B Biol. Sci. 280:20132451.

Svardal H., Quah F.X., Malinsky M., Ngatunga B.P., Miska E.A., Salzburger W., Genner M.J., Turner G.F., Durbin R. 2020. Ancestral Hybridization Facilitated Species Diversification in the Lake Malawi Cichlid Fish Adaptive Radiation. Mol. Biol. Evol. 37:1100–1113.

Swofford D.L. 2003. PAUP*. Phylogenetic Analysis Using Parsimony (* and Other Methods).

Tange O. 2011. GNU Parallel - The Command-Line Power Tool.

Taylor S.A., Larson E.L. 2019. Insights from genomes into the evolutionary importance and prevalence of hybridization in nature. Nat. Ecol. Evol. 3:170–177.

Than C., Degnan J.H., Nakhleh L. 2011. Coalescent Histories on Phylogenetic Networks and Detection of Hybridization Despite Incomplete Lineage Sorting. Syst. Biol. 60:138–149.

Tolesa Z., Bekele E., Tesfaye K., Ben Slimen H., Valqui J., Getahun A., Hartl G.B., Suchentrunk F. 2017. Mitochondrial and nuclear DNA reveals reticulate evolution in hares (*Lepus* spp., Lagomorpha, Mammalia) from Ethiopia. PLoS One.

12:e0180137.

Vanderpool D., Minh B.Q., Lanfear R., Hughes D., Murali S., Harris R.A., Raveendran M., Muzny D.M., Gibbs R.A., Worley K.C., Rogers J., Hahn M.W. 2020. Primate phylogenomics uncovers multiple rapid radiatio. bioRxiv. https://doi.org/10.1101/2020.04.15.043786

Wang R.J., Hahn M.W. 2018. Speciation genes are more likely to have discordant gene trees. Evol. Lett. 2:281–296.

Wen D., Yu Y., Hahn M.W., Nakhleh L. 2016. Reticulate evolutionary history and extensive introgression in mosquito species revealed by phylogenetic network analysis. Mol. Ecol. 25:2361–2372.

White J.A. 1991. North American Leporinae (Mammalia: Lagomorpha) from late Miocene (Clarendonian) to latest Pliocene (Blancan). J. Vertebr. Paleontol. 11:67–89.

Yamada F., Takaki M., Suzuki H. 2002. Molecular phylogeny of Japanese Leporidae, the Amami rabbit *Pentalagus furnessi*, the Japanese hare *Lepus brachyurus*, and the mountain hare *Lepus timidus*, inferred from mitochondrial DNA sequences. Genes Genet. Syst. 77:107–16.

Yang Z. 2007. PAML 4: Phylogenetic analysis by maximum likelihood. Mol. Biol. Evol. 24:1586–1591.

Yu Y., Degnan J.H., Nakhleh L. 2012. The Probability of a Gene Tree Topology within a Phylogenetic Network with Applications to Hybridization Detection. PLoS Genet. 8:1002660.

Yu Y., Dong J., Liu K.J., Nakhleh L. 2014. Maximum likelihood inference of reticulate evolutionary histories. Proc. Natl. Acad. Sci. 111:16448–16453.

Yu Y., Nakhleh L. 2015. A maximum pseudo-likelihood approach for phylogenetic

networks. BMC Genomics. 16:S10.

Zhang C., Rabiee M., Sayyari E., Mirarab S. 2018. ASTRAL-III: Polynomial time species tree reconstruction from partially resolved gene trees. BMC Bioinformatics. 19:153.

Zimova M., Hackländer K., Good J.M., Melo-Ferreira J., Alves P.C., Mills L.S. 2018. Function and underlying mechanisms of seasonal colour moulting in mammals and birds: what keeps them changing in a warming world? Biol. Rev. 93:1478–1498.

1117

1118 **FIGURE LEGENDS**

1119

1120 **Fig. 1 - Hare (*Lepus* spp.) evolutionary history and biogeography. A)** The
1121 distribution of the 15 hare species studied here; **B)** Coalescent species tree estimated
1122 with *ASTRAL;* nodes with *ASTRAL* posterior probability equal to one, *ASTRAL* quartet
1123 score higher than 0.6, and *SVDquartets* bootstrap support higher than 90 are labeled; **C)**
1124 Maximum-likelihood phylogeny of *Lepus* showing ancestral range reconstructions. Pie
1125 charts show proportional likelihoods that the common ancestral was distributed in North
1126 America (blue), Eurasia (green) or Africa (red). Asterisks depict nodes with equivocal
1127 reconstruction of ancestor distribution.

1128

1129 **Fig. 2 - The hare (*Lepus* spp.) species tree is underlined by extensive gene tree**
1130 **incongruence.** Split network constructed from 8889 gene trees (5% threshold) shows
1131 discordance among the gene tree topologies (cuboid structures represent alternative
1132 topologies) in deeper nodes of the species tree. Species are marked with colors
1133 corresponding to the continents where they are distributed.

1134

1135 **Fig. 3 – Admixture events are distributed across the hare (*Lepus* spp.) species tree.**
1136 The branch-specific statistic $f_b(C)$ represents excess allele sharing between branches *b*
1137 (y-axis) and *C* (x-axis) of the species tree in Figure 1. The orange gradient represents
1138 the $f_b(C)$ score, gray represents tests not consistent with the species tree and asterisks
1139 denote block jackknifing significance at $P \leq 0.05$ (after Bonferroni correction). Tips of
1140 the tree are colored according to their current distribution (two colors represent
1141 distribution in both areas), and ancestral tips (dashed gray and labeled with letters) are

1142 colored according to the ancestral reconstruction of distribution areas from Figure 1
1143 (two colors represent equivocal inference of the two-character states). Ancestral tips are
1144 labeled from A to L corresponding to labels in Supplementary Table S11.
1145
1146 **Fig. 4 – Admixture proportions decrease with genetic divergence between**
1147 **allopatric species.** We plot $f_b(C)$ values against exome-wide divergence (d_{xy}) for extant
1148 species pairs, coloring points when species have overlapping (sympatric/parapatric) or
1149 non-overlapping (allopatric) distributions. The tendency line represents a linear
1150 regression relating d_{xy} and $f_b(C)$ values calculated with function *lm()* in R.
1151
1152 **Fig. 5 – The impact of ancestral introgression on extant northern latitude species.**
1153 **A)** Events of past and recent admixture inferred in this study involving snowshoe,
1154 Alaskan hares, mountain hares and white-tailed jackrabbits. The arrow indicates the
1155 direction of ancestral introgression inferred by *PhyloNet*; **B)** Genomic distribution of
1156 ancestral blocks of introgression inferred as shared outliers windows among fraction of
1157 admixture (f_d) analysis testing for admixture among snowshoe hares and each one of the
1158 three other northern latitude species (orange), and blocks private to the analysis with
1159 Alaskan hares (blue) and white-tailed jackrabbits (black). Tests were run in 50 kb
1160 genomic sliding windows, and outlier windows are in the top 0.5% of the f_d distribution.
1161

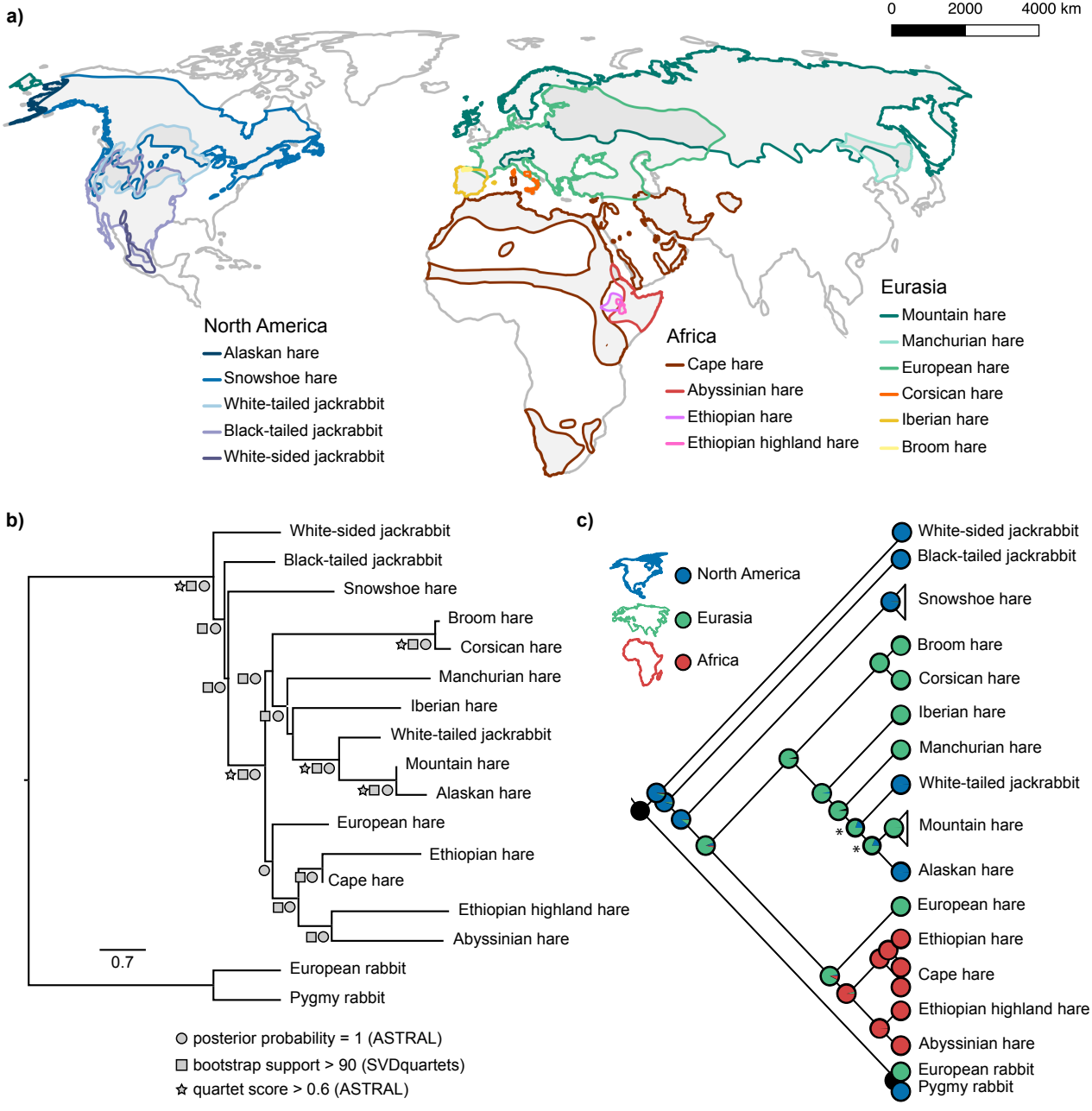
a)
0
2000
4000 km
North America
Alaskan hare
Snowshoe hare
White-tailed jackrabbit
Black-tailed jackrabbit
White-sided jackrabbit
Africa
Cape hare
Abyssinian hare
Ethiopian hare
Ethiopian highland hare
Eurasia
Mountain hare
Manchurian hare
European hare
Corsican hare
Iberian hare
Broom hare
b)
White-sided jackrabbit
Black-tailed jackrabbit
Snowshoe hare
Broom hare
Corsican hare
Manchurian hare
Iberian hare
White-tailed jackrabbit
Mountain hare
Alaskan hare
European hare
Ethiopian hare
Cape hare
Ethiopian highland hare
Abyssinian hare
0.7
European rabbit
Pygmy rabbit
posterior probability = 1 (ASTRAL)
bootstrap support > 90 (SVDquartets)
quartet score > 0.6 (ASTRAL)
c)
North America
Eurasia
Africa
White-sided jackrabbit
Black-tailed jackrabbit
Snowshoe hare
Broom hare
Corsican hare
Iberian hare
Manchurian hare
White-tailed jackrabbit
Mountain hare
Alaskan hare
European hare
Ethiopian hare
Cape hare
Ethiopian highland hare
Abyssinian hare
European rabbit
Pygmy rabbit

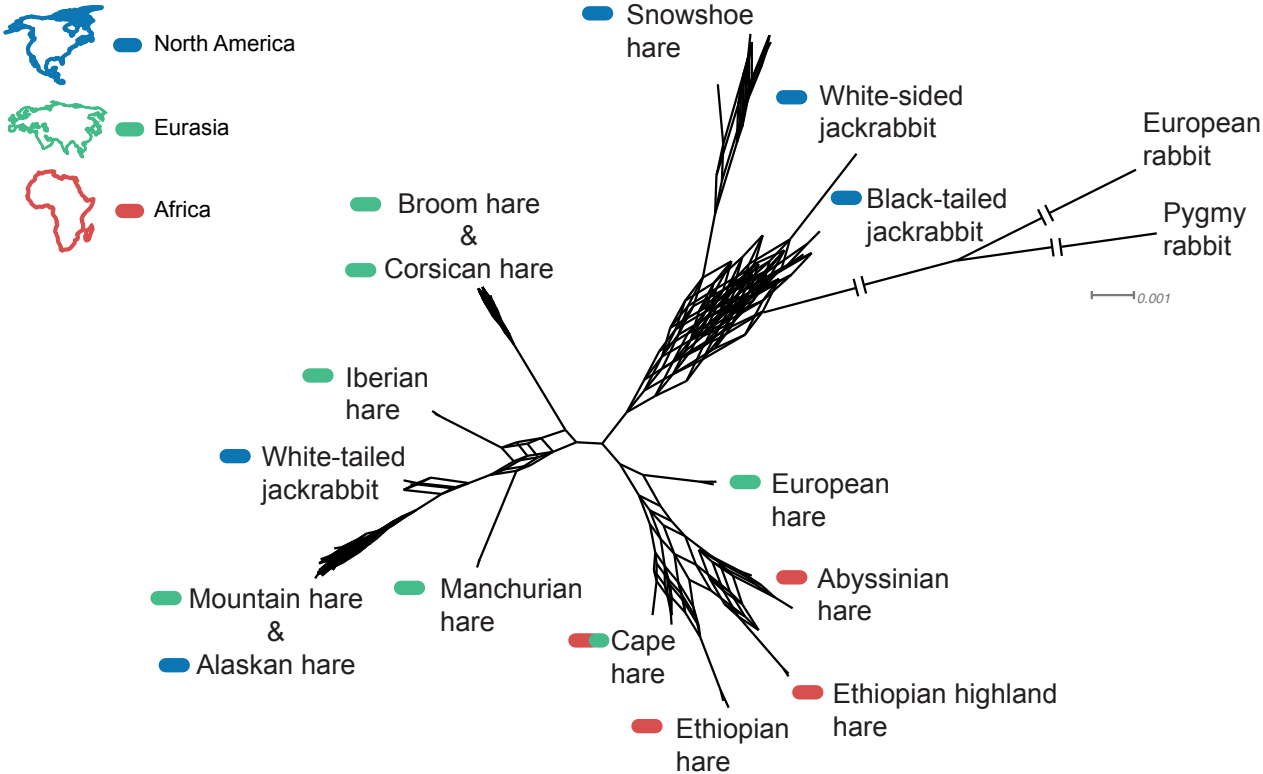
North America
Eurasia
Africa
Snowshoe hare
White-sided jackrabbit
European rabbit
Black-tailed jackrabbit
Pygmy rabbit
0.001
Broom hare
&
Corsican hare
Iberian hare
White-tailed jackrabbit
European hare
Abyssinian hare
Mountain hare
&
Alaskan hare
Manchurian hare
Cape hare
Ethiopian highland hare
Ethiopian hare

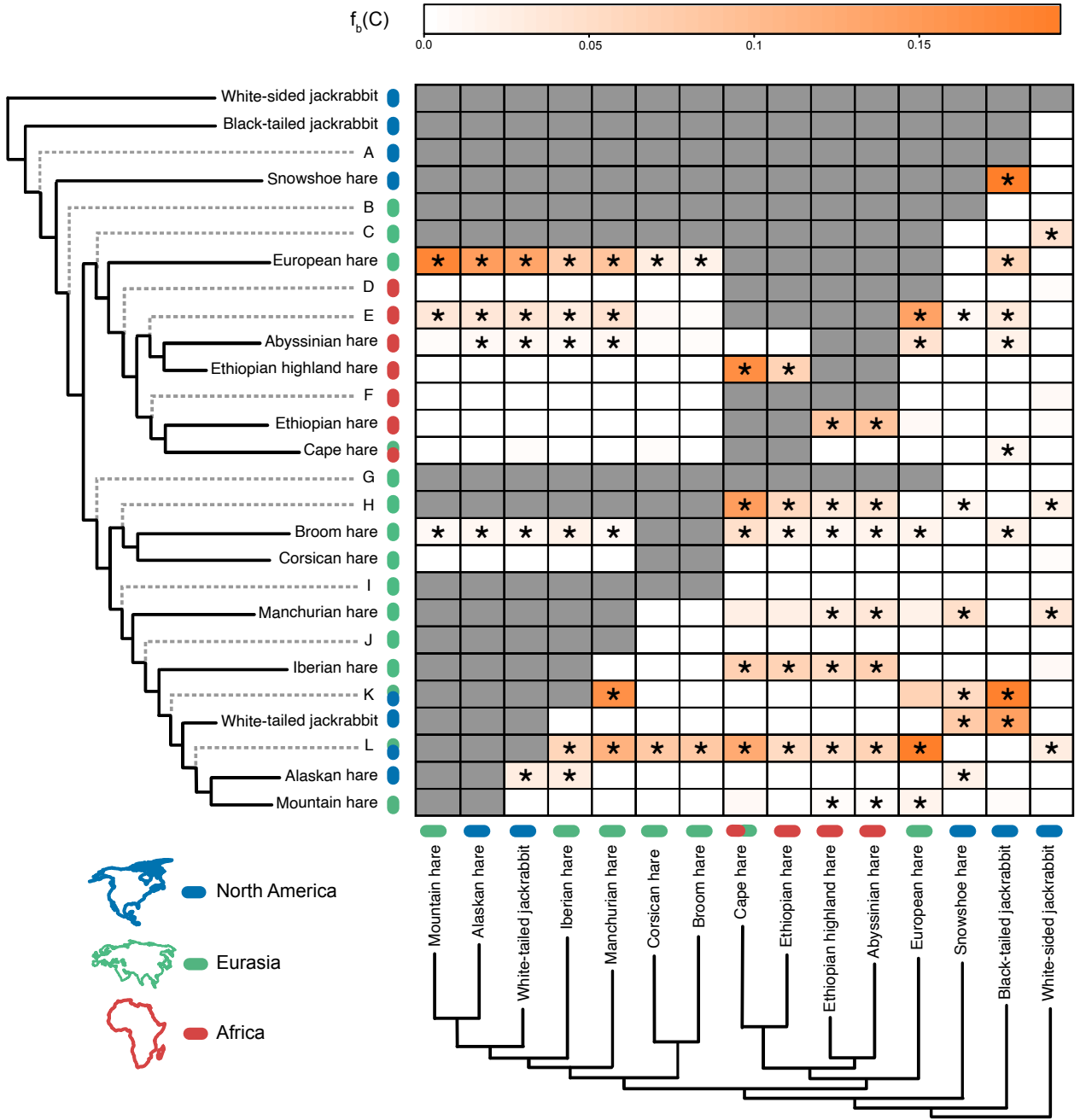
$f_b(C)$
0.0
0.05
0.1
0.15
White-sided jackrabbit
Black-tailed jackrabbit
A
Snowshoe hare
B
C
European hare
D
E
Abyssinian hare
Ethiopian highland hare
F
Ethiopian hare
Cape hare
G
H
Broom hare
Corsican hare
I
Manchurian hare
J
Iberian hare
K
White-tailed jackrabbit
L
Alaskan hare
Mountain hare
Mountain hare
Alaskan hare
White-tailed jackrabbit
Iberian hare
Manchurian hare
Corsican hare
Broom hare
Cape hare
Ethiopian hare
Ethiopian highland hare
Abyssinian hare
European hare
Snowshoe hare
Black-tailed jackrabbit
White-sided jackrabbit
North America
Eurasia
Africa

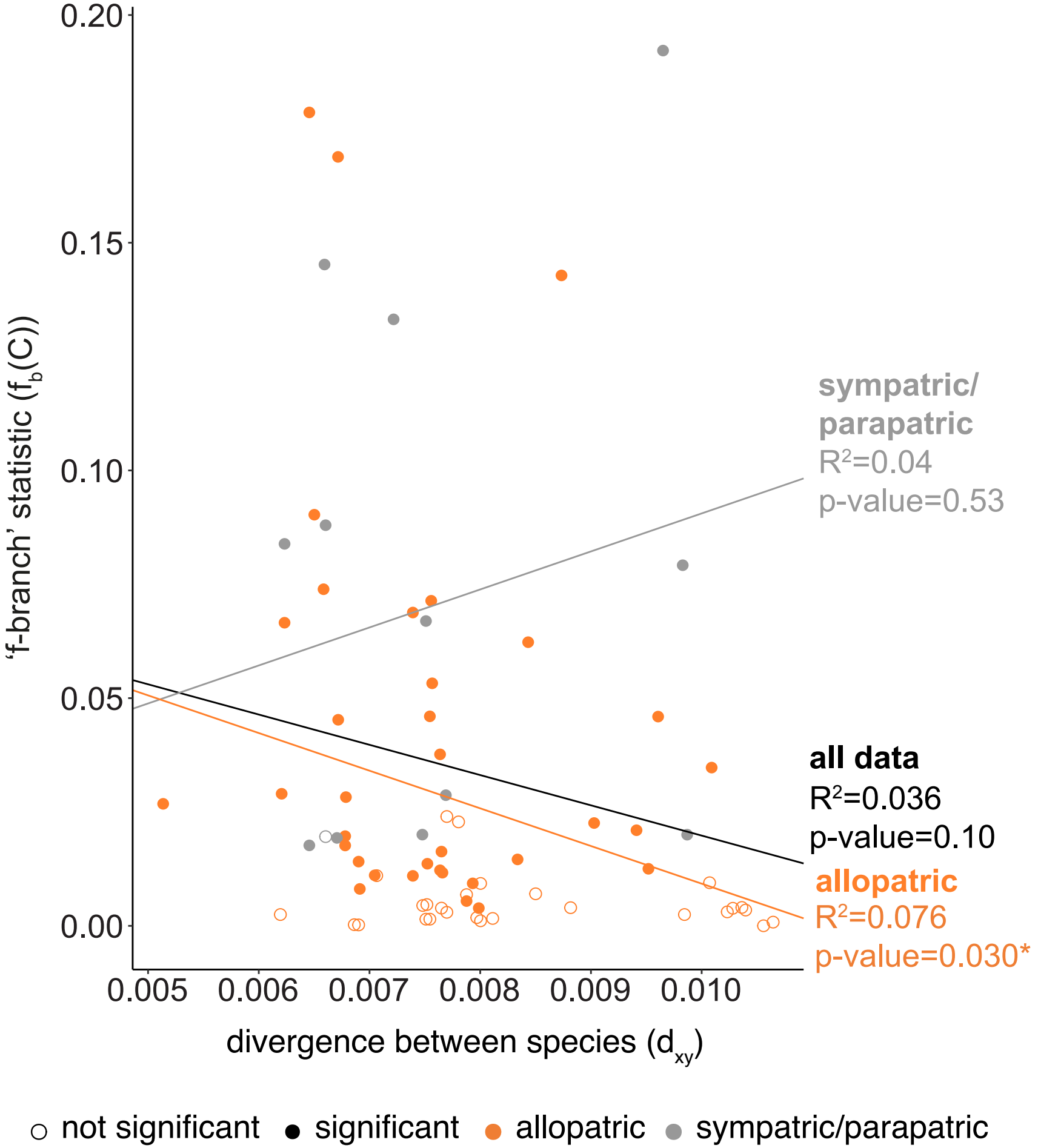
0.20
0.15
0.10
0.05
0.00
'f-branch' statistic ($f_b(C)$)
0.005
0.006
0.007
0.008
0.009
0.010
divergence between species (d_{xy})
sympatric/
parapatric
R^2=0.04
p-value=0.53
all data
R^2=0.036
p-value=0.10
allopatric
R^2=0.076
p-value=0.030*
not significant
significant
allopatric
sympatric/parapatric

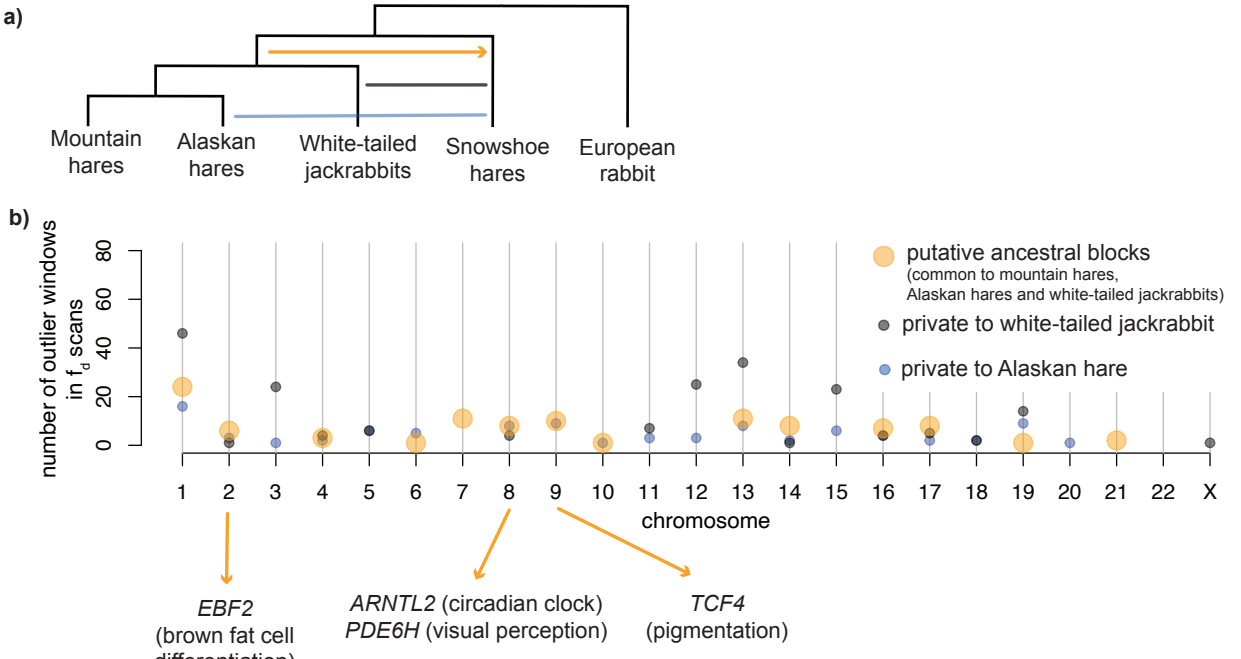
a)
Mountain hares
Alaskan hares
White-tailed jackrabbits
Snowshoe hares
European rabbit
b)
number of outlier windows in f_d scans
0
20
40
60
80
putative ancestral blocks
(common to mountain hares, Alaskan hares and white-tailed jackrabbits)
private to white-tailed jackrabbit
private to Alaskan hare
1 2 3 4 5 6 7 8 9 10 11 12 13 14 15 16 17 18 19 20 21 22 X
chromosome
EBF2 (brown fat cell differentiation)
ARNTL2 (circadian clock)
PDE6H (visual perception)
TCF4 (pigmentation)